Microbiome

RESEARCH

Open Access

Microbiota alterations leading to amino acid deficiency contribute to depression in children and adolescents

Teng Teng[1†], Fang Huang[1,2†], Ming Xu[3,4†], Xuemei Li[1†], Lige Zhang[1], Bangmin Yin[1], Yuping Cai[5], Fei Chen[1], Luman Zhang[1], Jushuang Zhang[2], Aoyi Geng[2], Chengzhi Chen[6,7], Xiaofei Yu[8], Jing Sui[3], Zheng-Jiang Zhu[5], Kai Guo[2,9*], Chenhong Zhang[10*] and Xinyu Zhou[1*]

Abstract

Background Major depressive disorder (MDD) in children and adolescents is a growing global public health concern. Metabolic alterations in the microbiota-gut-brain (MGB) axis have been implicated in MDD pathophysiology, but their specific role in pediatric populations remains unclear.

Results We conducted a multi-omics study on 256 MDD patients and 307 healthy controls in children and adolescents, integrating plasma metabolomics, fecal metagenomics, and resting-state functional magnetic resonance imaging (rs-fMRI) of the brain. KEGG enrichment analysis of 360 differential expressed metabolites (DEMs) indicated significant plasma amino acid (AA) metabolism deficiencies (p-value < 0.0001). We identified 58 MDD-enriched and 46 MDD-depleted strains, as well as 6 altered modules in amino acid metabolism in fecal metagenomics. Procrustes analysis revealed the association between the altered gut microbiome and circulating AA metabolism (p-value = 0.001, M^2 = 0.932). Causal analyses suggested that plasma AAs might mediate the impact of altered gut microbiota on depressive and anxious symptoms. Additionally, rs-fMRI revealed that connectivity deficits in the frontal lobe are associated with depression and 22 DEMs in AA metabolism. Furthermore, transplantation of fecal microbiota from MDD patients to adolescent rats induced depressive-like behaviors and 14 amino acids deficiency in the prefrontal cortex (PFC). Moreover, the dietary lysine restriction increased depression susceptibility in adolescent rats by reducing the expression of excitatory amino acid transporters in the PFC.

Conclusions Our findings highlight that gut microbiota alterations contribute to AAs deficiency, particularly lysine, which plays a crucial role in MDD pathogenesis in children and adolescents. Targeting AA metabolism may offer novel therapeutic strategies for pediatric depression.

Keywords Depression, Amino acid, MGB axis, Children and adolescents, Microbiota, Glutaminergic synapse

†Teng Teng, Fang Huang, Ming Xu and Xuemei Li contributed equally contributed equally to this manuscript.

*Correspondence:
Kai Guo
kaiguo@med.umich.edu
Chenhong Zhang
zhangchenghong@situ.edu.cn
Xinyu Zhou
zhouxinyu@cqmu.edu.cn
Full list of author information is available at the end of the article

Introduction

Major depressive disorder (MDD) in children and adolescents significantly contributes to the global burden of disease [1], affecting approximately 4–5% of individuals in this age group [2]. The social and functional limitations experienced by young individuals diagnosed with MDD are more severe than those observed in adults [3]. Additionally, they face a heightened risk of suicide, a leading cause of mortality among adolescents aged 15–19 years [4], which may be attributed to unique neurodevelopmental vulnerabilities, including the hypothalamic–pituitary–adrenal axis, serotonergic system, signal transduction pathways, and inflammatory factors [5]. Moreover, while most antidepressants are effective in treating MDD in adults, they do not exhibit the same efficacy in children and adolescents and may even increase the risk of suicide, as seen with venlafaxine [6]. Therefore, it is crucial to conduct comprehensive research into the age-specific neurobiological mechanisms underlying depression in children and adolescents to develop more effective and safer treatment strategies for this vulnerable population.

The gastrointestinal tract functions as an anaerobic bioreactor, harboring a diverse microbiota. The microbiota-gut-brain (MGB) axis has emerged as a crucial regulator of various health and disease aspects [7, 8]. Increasing evidence has indicated that gut microbiota modulates neurodevelopment through microbial metabolites (e.g., SCFAs), which regulate blood–brain barrier integrity via tight junction proteins (occludin, claudin-5) and microglial maturation via FFAR2 signaling, as well as alterations in microbiota dependent oxytocin, serotonin, and NAMD receptor function, contributing to neuropsychiatric disorders such as ASD and mood disorders [9]. Moreover, substantial evidence links disrupted gut microbiome to depression, such as depleted *Faecalibacterium* and enriched *Eggerthella* [10, 11]. Recent research has indicated that *Bifidobacterium longum* ameliorate depressive-like behaviors in mouse models of depression by homovanillic acid [12]. In addition, *Lactobacillus Plantarum*, a strain known to produce high levels of γ-aminobutyric acid, has been observed to offer protection against depression-like states in the context of *Drosophila* [13]. The composition of the gut microbiota changes with age, and children and adolescents are more susceptible to environmental factors than adults, whose microbiota tends to be more stable [14]. Our previous study revealed age-specific metabolic divergence in MDD, with polyunsaturated fatty acids and purine metabolism predominating in children and adolescents versus tryptophan metabolism in adults, suggesting a potential mediating role of age-stratified gut microbiota in these differential metabolic pathways [15]. However, research on the role of the MGB axis and its impact on the metabolic processes of children and adolescents with depression remains limited.

In this study, our central hypothesis is that alterations in the gut microbiota induce metabolic dysregulation in the MGB axis in a brain region-specific manner, thereby contributing to the development of depressive symptoms. To test this hypothesis, we conducted a comprehensive multi-omics analysis using large-scale untargeted mass spectrometry of plasma, metagenomic sequencing of feces, and resting-state functional magnetic resonance imaging (rs-fMRI) of the brain to elucidate the MGB axis in the context of depression in children and adolescents. We integrated multi-omics data to explore the potential interactive connections between the gut microbiota and the brain through metabolic pathways. Additionally, we investigated potential causal mechanisms through fecal microbiota transplantation (FMT) from children and adolescents with MDD or healthy controls (HCs) to antibiotic-treated (Abx) adolescent rats, as well as the dietary lysine restriction experiment in an adolescent depression rat model (Fig. S1). The results support the hypothesis that alterations in the gut microbiota, leading to a deficiency in amino acids (AAs), contribute to the pathogenesis of depression in children and adolescents.

Methods

Subject recruitment

The protocol of this study was reviewed and approved by the Ethics Committee of the First Affiliated Hospital of Chongqing Medical University (#2020–684). The written informed consent was signed by both the participant and their legal guardian. The study population consisted of 563 children and adolescents, ranging in age from 10 to 18 years, who were enrolled, including 256 patients with MDD and 307 healthy controls (HCs, for demographic and clinical characters, please see Table 1). Plasma samples were collected from all 563 participants, while fecal samples were limited to a subset of 83 patients with MDD and 58 HCs (for demographic and clinical characters, please see Table S1). In addition, a subset of 111 patients with MDD and 51 HCs participated in the MRI session (for demographic and clinical characters, please see Table S2). All patients with MDD who met the diagnostic criteria for MDD according to the Diagnostic and Statistical Manual of Mental Disorders, 5th Edition (DSM-5), were recruited from the First Affiliated Hospital of Chongqing Medical University. The diagnosis was established through face-to-face structured clinical interviews conducted by two experienced psychiatrists who had undergone a formal consistency assessment to ensure diagnostic accuracy and reliability. HCs were recruited through community or school advertisements

Table 1 Summary of clinical parameters of all individuals from MDD and HCs

Parameters	HCs ($n = 307$)	MDD ($n = 256$)	p-value
Age (years)	15.3 ± 1.8	15.4 ± 1.7	0.76 [a]
BMI (kg/m^2)	20.3 ± 3.6	20.2 ± 3.0	0.98 [a]
Gender (*N* and % female)	207 (67.4%)	188 (73.4%)	0.12 [b]
HAMD-24	2.1 ± 1.6	26.2 ± 8.6	< 0.001 [a]
HAMA-14	1.2 ± 1.2	16.5 ± 7.2	< 0.001 [a]

Summary statistics: distribution of the variable in HCs and MDD, measured as mean ± SD for continuous variables, or as numbers and percentages for dichotomous variables

HCs, health controls; *MDD*, major depressive disorder; *BMI*, body mass index; *HAMA-24*, the 24-item Hamilton Depression Rating Scale; *HAMA-14*, the 14-item Hamilton Anxiety Rating Scale; *SD*, standard deviation

[a] Mann-Whitney *U* test

[b] Chi-square test

and underwent the same structured clinical interviews to confirm the absence of any DSM-5 psychiatric disorder. Participants in both groups were free of physical illness or illicit drug use and were not currently pregnant or lactating. They also had no contraindications to having a magnetic resonance imaging (MRI) scan. The 24-item Hamilton Depression Rating Scale (HAMD-24) and the 14-item Hamilton Anxiety Rating Scale (HAMA-14) were used to assess the severity of depression and anxiety symptoms, respectively. All enrolled MDD participants presented depressive symptoms (HAMD-24 ≥ 8), with most (77.7%) showing moderate to severe severity (HAMD-24 ≥ 20). Interviews and assessments were conducted by trained psychiatrists in the participants' native language (Chinese), and parental involvement was permitted based on participant preference. In addition, other relevant demographic and clinical information, such as age, sex, and body mass index (BMI), was collected through face-to-face interviews at the time of enrollment for all participants, including both MDD patients and HCs.

Plasma and fecal sample collection

All the 563 blood samples were taken from the participants between 8:00 AM and 12:00 AM by venipuncture and were immediately placed in EDTA-coated (anticoagulant) tubes (Becton, Dickinson and Company, USA). The tubes were then centrifuged for 10 min at 3000 rpm and 4 °C. After centrifugation, the plasma was separated and stored at − 80 °C until metabolomic profiling. Similarly, all 141 fecal samples were collected, using sterile, DNA-free devices (Bobeili, China), mixed with 10% glycerol (Solarbio, China), rapidly frozen in ice, and then stored at − 80 °C until shotgun sequencing. Samples were collected at a hospital or home, and homogenization was performed before storage to ensure representative sampling.

Plasma metabolic profiling and analysis of MDD patients and HCs

Plasma metabolic profiling was performed on all participants, including 256 patients with MDD and 307 HCs. The liquid chromatography-mass spectrometry (LC–MS) analysis protocol followed that described in our previous publication [16]. Data acquisition was performed using a Thermo Scientific Vanquish UHPLC system coupled to a Thermo Scientific Orbitrap Exploris 480. LC separation utilized a Waters ACQUITY UPLC BEH Amide column and a Kinetex C18 column, maintained at 25 °C. For HILIC, mobile phase A was 25 mM NH4OH (Sigma-Aldrich, USA) and NH4OAc (Sigma-Aldrich, USA) in water, while phase B was acetonitrile. The flow rate was 0.5 mL/min with a gradient setup. Reverse phase liquid chromatography (RPLC) analysis used 0.01% acetic acid in water as phase A and a 1:1 mixture of isopropyl alcohol and acetonitrile as phase B with a flow rate of 0.3 mL/min. Samples underwent full MS scan mode with polarity switching, and quality control samples were analyzed in information-dependent acquisition mode. The data processing protocol followed the protocol described in our previous publications [17, 18]. Data processing used ProteoWizard (version 3.0.20360) for conversion to mzXML format, followed by peak detection and alignment with the "xcms" package. Missing value imputation and normalization were performed using MetFlow software (http://metflow.zhulab.cn/). Metabolite peaks with RSDs < 30% in QC samples were analyzed. Metabolite annotation was done using MetDNA (version 1.2.2; http://metdna.zhulab.cn/), adjusting parameters based on chromatography mode and collision energy settings. Differentially expressed metabolites between MDD and HCs were identified using multivariate and univariate analyses in R (version 4.1.2) and SIMCA-P (version 11.0). Principal component analysis (PCA) assessed overall metabolic changes, while partial least squares discrimination analysis (PLS-DA) maximized group differences to identify key metabolites. Univariate analyses employed Wilcoxon-Mann–Whitney tests with FDR adjustments. Criteria for differentially expressed metabolites included VIP > 1 and p-value < 0.05. Volcano plots and heatmaps illustrated the metabolite profiles. Functional enrichment analysis was conducted using the richR package (https://github.com/hurlab/richR). Recursive feature elimination (RFE) identified relevant features, and random forest modeling assessed the performance of selected amino acids, with receiver operating characteristic (ROC) curves generated for evaluation. Please see the supplementary methods

for more details on the plasma metabolic profiling and analysis.

Metagenomic sequencing and analysis

Metagenomic sequencing and analysis were performed on a subset of 83 patients with MDD and 58 HCs. Fecal DNA was extracted using the PF Mag-Bind Soil DNA Kit (Omega Bio-tek, USA), with concentration and purity assessed via TBS-380 and NanoDrop2000, respectively, and quality-checked by agarose gel electrophoresis. DNA was stored at −80 °C prior to shotgun metagenomic sequencing. The DNA was fragmented to ~400 bp with the Covaris M220 (Gene Company Limited, China) and prepared for paired-end sequencing using the NEXTFLEX Rapid DNA-Seq Kit (Bioo Scientific, USA) on the Illumina NovaSeq 6000 (Illumina Inc., USA). Sequence data is available in the NCBI Short Read Archive (Accession Number: SUB14742785). Raw sequencing data were processed with fastp (version 0.23.2) [19] for clean data preparation. To exclude host contamination, clean reads were aligned against a host database using Bowtie2 [20]. High-quality paired-end reads were de novo assembled using Megahit (version 1.2.9) [21]. ORF sequences were predicted with PRODIGAL (version 2.6.3) [22], and redundant sequences were filtered with CD-HIT (version 4.8.1) [23]. Gene reads were quantified using SOAP2 (version 2.21) [24], and unigenes were established by excluding low-coverage genes. Gene abundance was then calculated for basic statistical analysis. The final gene set (Unigenes) for further analysis can be obtained by filtering out the genes with less than two reads in each sample. Unigenes were compared to NCBI NR sequences using DIAMOND [25] software (version 2.0.8.146, https://github.com/bbuchfink/diamond/), and the LCA algorithm was applied for taxonomic classification. Gene abundance data were extracted at various taxonomic ranks. Unigenes were also compared to the Kyoto Encyclopedia of Genes and Genomes (KEGG) database for functional analysis to determine gene counts for different functions across samples. Binning was conducted using mmseqs2 [26] software (version 13.45111, https://github.com/soedinglab/MMseqs2) to create a unique scaftigs collection. Bowtie2 was employed for read mapping, and metabat2 [27] (version 2.15, https://bitbucket.org/berkeleylab/metabat) facilitated the binning process, both for single and mixed samples. Results were merged using dRep [28] (version 3.2.0, https://github.com/MrOlm/drep), and bin completeness and contamination were assessed with CheckM [29] (version 1.1.3, https://github.com/Ecogenomics/CheckM). Bins with >75% completeness and <10% contamination were retained for annotation via gtdb-tk [30] (version 1.7.0, https://github.com/Ecogenomics/GTDBTk, database version, 202). PERMANOVA estimated the contributions of clinical factors across different omics data. Spearman correlations were used for interactions between clinical parameters and metabolomics/microbiome data. Alpha diversity was assessed with the Shannon index, while beta diversity was analyzed via principal component analysis (PCoA) and PERMANOVA. The linear discriminant analysis effect size (LEfSe) identified significant microbiota characteristics. Bi-directional mediation analysis examined the effects of metabolites and microbiome on clinical parameters. Procrustes analysis assessed pattern similarity between metabolomic and microbiome data. Correlation networks for the gut microbiome were built using sparcc, and various network properties were calculated using R igraph package (version 2.0.3). Different criteria were tested for network reconstruction, focusing on node importance and connectivity metrics. Please see the supplementary methods for more details of the metagenomic sequencing and analysis.

MRI data acquisition and processing

MRI data analysis was performed on a subset of 111 patients with MDD and 51 HCs. After image acquisition using a Siemens Magnetom Skyra 3.0-T scanner with a 32-channel head coil, structural and functional images were preprocessed with fMRIPrep 20.2.5 (RRID: SCR_016216) [31], which is based on Nipype 1.6.1 (RRID: SCR_002502) [32]. The following descriptions of fMRIPrep's preprocessing workflows are based on boilerplate distributed with the software covered by "no rights reserved" (CC0) license. Internal operations of fMRIPrep use Nilearn 0.6.2 (RRID: SCR_001362) [33], ANTs 2.3.3 (RRID: SCR_004757), FSL 5.0.9 (RRID: SCR_002823), AFNI 20160207 (RRID: SCR_005927), and FreeSurfer 6.0.1 (RRID: SCR_001847). T1w images were corrected for intensity non-uniformity (INU) using *N4BiasFieldCorrection* [34] distributed with ANTs and were used as T1-references. Brain tissue segmentation of cerebrospinal fluid (CSF), white matter (WM), and gray matter (GM) was performed on the brain-extracted T1w using *fast* [35]. Volume-based spatial normalization to the ICBM 152 Nonlinear Asymmetrical template version 2009c (MNI152 NLin2009cAsym, RRID:SCR_008796) [36] was performed through nonlinear registration with *antsRegistration* [37], using brain-extracted versions of both T1w volume and the T1w template. Functional images were motion corrected with respect to a BOLD reference volume (which had firstly been generated via a custom methodology of fMRIPrep) using FSL's *mcflirt* [38] and slice-time corrected using AFNI's *3 dTshift* [39]. A deformation field to correct susceptibility distortions was estimated using fMRIPrep's field map-less approach [40, 41]. The BOLD reference was

then co-registered to the T1w image using FSL's *flirt* [42] with the boundary-based registration [43] cost function. Motion correcting transformations, susceptibility-distortion-correcting warp, BOLD-to-T1w transformation, and T1w-to-template (MNI152 NLin2009cAsym) warp were concatenated and applied in a single step using *antsApplyTransforms* with Lanczos interpolation [44]. Framewise displacement (FD) and DVARS were calculated for each functional run, both using their implementations in Nipype [45]. After preprocessing and denoising, functional connectivity between each pair of brain regions (defined by Brainnetome atlas, details about the region definitions are available in TableS3 and https://atlas.brainnetome.org/bnatlas.html) was calculated as the Fisher *z*-transformed Pearson correlation coefficient between the mean regional residual BOLD time series, resulting a 246 ×246 weighted adjacent matrix for each participant. Connectome-based predictive modeling identified associations between functional connectivity and plasma metabolites through leave-one-out cross-validation. Significant correlations ($p < 0.0005$) were retained, yielding individual scores. A linear model explained the brain-metabolite relationship, with predictions made for each left-out participant. The selection rate of connections across iterations measured their predictive power. Similar analytical procedures could be found in these previous studies [46–48]. The primary statistics threshold was set to $F = 11.238$, approximately corresponding to p-value $= 0.001$. Finally, the family-wise error (FWER) corrected p-value was calculated for each connected component by 5000 random permutations with super-threshold edge count as the size measure. The spin-based permutation test is a conservative statistical method accounting for each lobe's different size and the spatial autocorrelation of brain structures (www.github.com/frantisekvasa/rotate_parcellation) [49, 50]. Specifically, the proportion of connections with metabolite associations was calculated as the test statistics for a given lobar-level network; the brain parcellation maps were projected onto a sphere, which was rotated 5000 times to create a null distribution of the test statistics for each lobar-level network. Lobar networks were considered to have significant enrichment if the empirical test statistic was in the top 5% of the null distribution, i.e., $p_{spin} < 0.05$ [51]. Please see the Supplementarymethods for more details of the MRI data acquisition and processing.

Animal experiment of fecal microbiota transplantation (FMT)

The experiments of rats in this study were approved by the Institutional Animal Care and Use Committee (IACUC) of Chongqing Medical University (approval number: IACUC-CQMU-2024–0040). Fecal samples were collected from 19 individuals with MDD and 19 HCs (for demographic and clinical characters, please see TableS4). Each sample was mixed, with 0.8 g of feces homogenized in 40 ml saline and centrifuged at 10,000 rpm for 20 min at 4 °C. Before storage, a bacterial viability quantification was conducted by BHI medium (Microbial SCI&TECH, China) and YCFAG medium (Hope Bio-Technology, China) to ensure a standardized microbial load in the fecal gavage solution. The supernatant was preserved with 15% glycerol and stored at −80 °C. In total, 24 specific pathogen-free (SPF) male adolescent Sprague–Dawley rats with postnatal day (PND) 21 days were obtained from Chongqing Medical University and housed individually under controlled conditions (12-h light/dark cycle, 22 ± 1 °C). After acclimatization, the rats were subjected to a 2-week treatment regimen of twice-daily oral gavage with 0.2 ml of a broad-spectrum antibiotic mixture (ampicillin 25 mg/ml, metronidazole 25 mg/ml, neomycin 25 mg/ml, vancomycin 12.5 mg/ml, amphotericin B 0.25 mg/ml). Following treatment, the rats were divided into two groups, receiving oral gavage of 10 μl/g of fecal supernatant from either MDD patients ($n = 12$) or HCs ($n = 12$). The bacterial load in each fecal sample after FMT was quantified by qPCR targeting total bacterial 16S rRNA gene copies. Antibiotic-treated (Abx) rats were individually housed in sterile isolators supplied with filtered sterile air. All food (sterilized by cobalt-60 irradiation), water (autoclaved), and bedding (autoclaved) provided were sterile. Sample preparation and transplantation were conducted within a biosafety cabinet using sterile instruments, with researchers wearing sterile gowns, gloves, and masks to maintain aseptic conditions and prevent microbial contamination throughout the experiments. Body weight was measured weekly. To ensure consistency, daily gavage of fecal supernatant was performed at 9:00 AM for 2 weeks, and behavioral tests, including sucrose preference test (SPT), open field test (OFT), elevated plus-maze test (EPM), forced swim test (FST), were performed from 8:00 PM at the end of transplantation. At sacrifice, following transcardial perfusion, fresh brain tissue was carefully extracted and immediately placed on ice (4 °C). The olfactory bulbs were removed, and the prefrontal cortex (PFC) was isolated by dissecting the anterior 1 mm of the frontal brain region using a scalpel. Samples from the PFC were then snap-frozen in liquid nitrogen and stored at −80 °C. The methodology employed in the behavioral tests has been described in detail in our earlier studies [52]. The details of the liquid chromatography-mass spectrometry (LC–MS) analysis have been reported in our previous studies [53]. The standard substance of 20 amino acids was employed to calculate the retention time and identify metabolites (TableS5). The same metagenome assembly

process should be used to generate the unigenes set, after which gene annotation was run through DIAMOND (version 2.0.8.146, https://github.com/bbuchfink/diamond/) on different reference databases (NR for taxonomy, KEGG for gene function annotation). The relative abundance of the FMT samples' metagenome-assembled genomes (MAGs) was calculated based on the mapping of reads to the same MAGs set as the host, followed by the same statistical analysis process, including PCoA analysis. Please see the supplementary methods for more details on the animal experiment of FMT.

The dietary lysine restriction in adolescent chronic unpredictable mild stress (CUMS) rats

The CUMS protocol has been previously described in detail in our laboratory [52]. A total of 48 SPF male adolescent Sprague–Dawley rats (PND 21 days) were obtained from Chongqing Medical University and housed under controlled conditions (12-h light/dark cycle, 22 ± 1 °C). After 1 week of acclimatization, the rats were randomly divided into four groups: controls with 100% dietary lysine (CON + L100; $n = 8$), controls with 70% dietary lysine (CON + L70; $n = 8$), CUMS with 100% dietary lysine (CUMS + L100; $n = 9$), and CUMS with 70% dietary lysine (CUMS + L70; $n = 9$). Dietary lysine was administered for four weeks. Rats in the CUMS groups were subjected to two mild random stressors daily for four weeks, with no repeated stressors on consecutive days. Body weight was recorded weekly, and behavioral tests (SPT, OFT, EPM, and FST) were conducted after the dietary intervention. At sacrifice, PFC samples were collected, snap-frozen in liquid nitrogen, and stored at − 80 °C. RNA from PFC tissue was extracted using Trizol (Invitrogen, USA) and evaluated with a NanoDrop and an Agilent 2100 bioanalyzer (Thermo Fisher Scientific, USA). RNA libraries were constructed and sequenced by BGI-Shenzhen, involving cDNA synthesis, PCR amplification, and the creation of DNA nanoballs (DNBs) for sequencing on the DNBSEQ platform. Sequencing data underwent quality filtering and alignment to the reference genome. Gene expression levels were quantified, and differentially expressed genes (DEGs) were identified with a false discovery rate (FDR)-adjusted Padj cutoff of 0.05 and a minimum fold change of 2. KEGG enrichment analyses were performed on identified DEGs with a p-value cutoff of 0.05. RNA extraction from PFC tissues was carried out using the TRIzol method, followed by cDNA synthesis with the PrimeScript™ RT reagent Kit (RR047 A, Japan). qPCR was performed using the SYBR-Green master mix (MedChemExpress, USA), normalizing data against β-actin and calculating relative gene expression with the 2-ΔΔCT method. Further details regarding the primers can be found in TableS6. PFC tissue was homogenized in RIPA buffer (Beyotime Biotechnology, China) containing protease inhibitors (MedChemExpress, China). After centrifugation, protein content was quantified, and samples were separated into gels and transferred to PVDF membranes. Membranes were blocked, incubated overnight with specific antibodies (EAAT2 [ab205248, Abcam, UK] and EAAT3 [ab288441, Abcam, UK]), and then washed and incubated with HRP-conjugated antibodies (1:3000, CST, USA). Blots were developed with ECL Prime reagent (GE Healthcare), imaged, and densitometry analysis was performed using ImageJ software (NIH, Bethesda). Please see the supplementary methods for more details on the animal experiment of the dietary lysine restriction in adolescent CUMS rats.

Results

The deficiency of plasma amino acids in children and adolescents with MDD

To investigate the metabolic characteristics of depression in children and adolescents, we recruited 256 individuals in MDD, of whom 188 (73.4%) were female, with an average age of 15.4 ± 1.7 years, and a mean body mass index (BMI) of 20.2 ± 3.0 kg/m^2; as well as 307 healthy controls, of whom 207 (67.4%) were female, with an average age of 15.3 ± 1.8 years and an average BMI of 20.3 ± 3.6 kg/m^2. Significant differences were observed in the scores of the 24-item Hamilton Depression Rating Scale (HAMD-24) (26.2 ± 8.6 vs. 2.1 ± 1.6; p-value < 0.001) and the 14-item Hamilton Anxiety Rating Scale (HAMA-14) (16.5 ± 7.2 vs. 1.2 ± 1.2; p-value < 0.001) between individuals with MDD and HCs (Table 1).

Plasma samples from all the participants were analyzed using hydrophilic interaction liquid chromatography-mass spectrometry (HILIC-MS) and reversed-phase liquid chromatography-mass spectrometry (RPLC-MS). Principal component analysis (PCA) and partial least square-discriminate analysis (PLS-DA) revealed significant metabolic alterations in children and adolescents with MDD compared to the HCs (Fig. 1A and Fig.S2). PLS-DA identified 360 differentially expressed metabolites (DEMs) by variable influence on projection (VIP) > 1 and false discovery rate (FDR) < 0.05 in Wilcoxon-Mann–Whitney test, with 297 downregulated and 63 upregulated plasma metabolites in MDD compared to HCs (Fig. 1B and TableS7). KEGG enrichment analysis of the DEMs identified 31 dysregulated pathways at level 2 (TableS8 and Fig.S3 A) and 122 pathways at level 3 (TableS9; the top 30 are shown in Fig.S3B). Amino acid metabolism was the most enriched KEGG level-2 pathway (Fig. 1C), involving 13 level-3 pathways, such as arginine and proline metabolism, tyrosine metabolism, and lysine biosynthesis (Fig. 1D). Additionally, significant

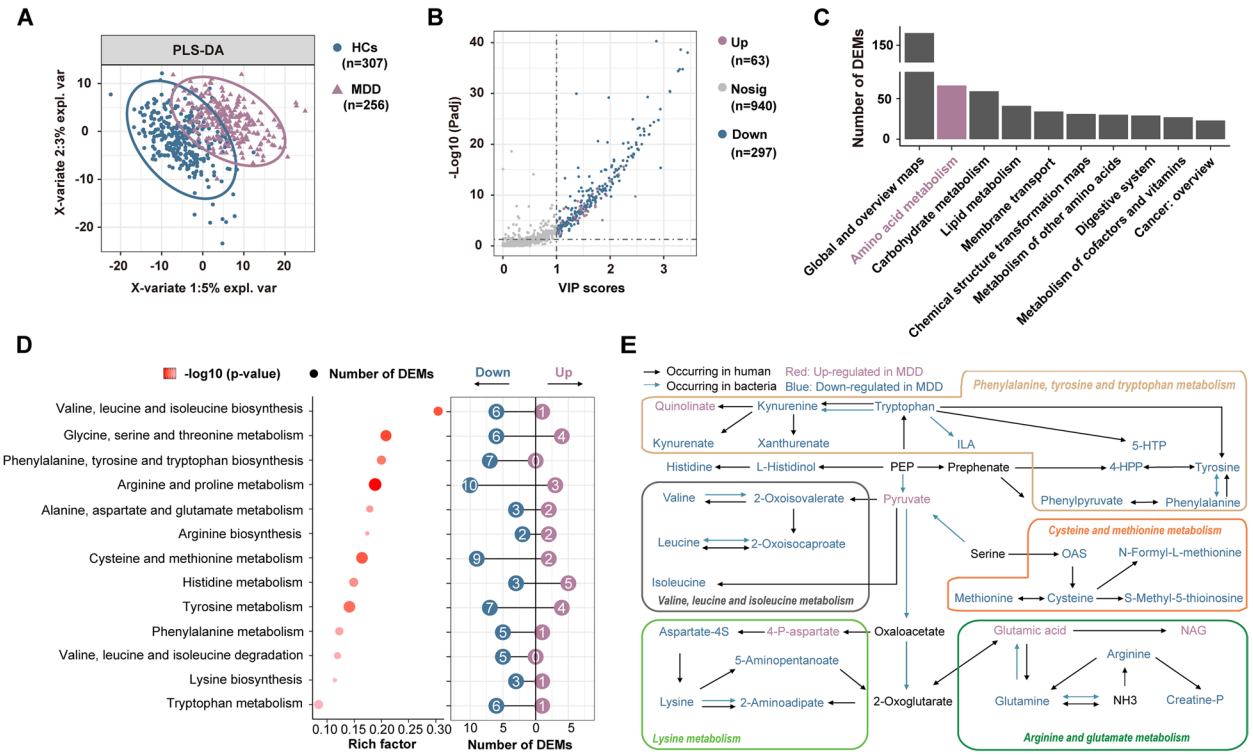

Fig. 1 The deficiency of plasma amino acids in children and adolescents with MDD. **A** A clear discrepancy of plasma metabolome between MDD patients ($n = 256$) and HCs ($n = 307$), revealed by Partial Least-Squares Discriminant Analysis (PLS-DA). **B** The volcano plot for all the 1300 identified metabolic features, including 63 up-regulated metabolites (red), 297 down-regulated metabolites (blue) and 940 non-significant metabolites (grey) in children and adolescents with MDD. **C** Kyoto Encyclopedia of Genes and Genomes (KEGG) enrichment analysis of all the 360 differentially expressed metabolites (DEMs) highlighted the amino acid metabolism was the most enriched KEGG level-2 functional pathway. **D** The KEGG enrichment analysis highlighted a total of 13 KEGG level-3 functional pathways in amino acid metabolism (left), and the number of differentially expressed metabolites (DEMs) in MDD patients are shown respectively (right), red dot color indicated the increased DEMs and blue dot indicated the decreased DEMs. **E** Representation of connections of phenylalanine, tyrosine, tryptophan, histidine, valine, leucine, isoleucine, cysteine, methionine, lysine, arginine, glutamic acid and glutamine metabolic pathways. ILA, Indole-3-lactic acid. 5-HTP, 5-Hydroxy-L-tryptophan. HPP, 4-Hydroxyphenylpyruvate. OAS, O-Acetyl-L-serine. Pcr, Creatine-P. NAG, N-Acetyl-L-glutamate. Data were sourced from the KEGG database

alterations were found in carbohydrate metabolism and digestive system pathways (Fig. 1C), which are known to be associated with depression [54]. Of the 20 amino acids (AAs) present in human peptides and proteins, 13 AAs were considerably dysregulated, including eight essential AAs (lysine, methionine, tryptophan, isoleucine, leucine, phenylalanine, valine and histidine), two conditionally essential AAs (cysteine and tyrosine), and three non-essential AAs (arginine, glutamine and glutamic acid). Most AAs were down-regulated, except for glutamic acid (TableS10), consistent with previous meta-analyses showing depletion of AAs like glutamine, tryptophan, methionine, and serine in MDD patients [55]. Of the 13 altered AAs, 8 AAs (arginine, tryptophan, glutamic acid, methionine, cysteine, tyrosine, lysine, and phenylalanine) were identified as being of particular interest due to their recapture by cross-validation of random forest with the highest accuracy (Fig.S3 C), which yielded an area under the receiver operating characteristic (AUROC) value of 0.978 in the training set (Fig.S3D). Moreover, 5-hydroxytryptophan, an intermediate metabolite of the EAA tryptophan in biosynthesis of serotonin, was downregulated in children and adolescents with MDD (FDR < 0.0001, VIP $= 2.49$; TableS7), suggesting that the increased demand for EAAs during growth may contribute to these alterations of these AAs in the context of depression, as they play a direct role or serve as precursors for neurotransmitters [56]. A summary of the alterations in amino acid metabolism is provided in Fig. 1E. Collectively, these findings indicate significant changes in plasma metabolomics in children and adolescents with MDD, particularly in AAs involved in neurotransmitter and protein synthesis.

Specific fecal microbial ecosystem in children and adolescents with MDD

Given the close association between host metabolism of AAs and gut microbiota, we performed metagenomic

sequencing of fecal samples from 83 MDD individuals (mean age, 15.4 ± 1.7 years; BMI, 20.6 ± 3.3 kg/m^2; 53 [63.9%] females) and 58 HCs individuals (mean age, 15.2 ± 2.1 years; BMI, 21.6 ± 4.3 kg/m^2; 33 [56.9%] females) in the above cohort (TableS1). On average, 1.00×10^8 high-quality reads per sample were obtained. After removing the reads from the human genome, an average of 8.03×10^7 microbial reads were retained and identified 4,770,497 non-redundant microbial genes from assembled contigs. A total of 282 genera and 521 species were identified through the construction of 1068 MAGs (TableS11).

Consistent with most previous findings in adult depression [57], no significant differences were observed between the two groups in the three indices used to evaluate the α-diversity of gut microbiota (Simpson, Chao1 and Shannon) (Fig. 2A). PCoA based on binomial distance showed a notable separation between the MDD and HCs groups at MAG-level (PERMANOVA, p-value = 0.001, Fig. 2B). We constructed a gut microbial co-occurrence network using SparCC with the relative abundance of 793 MAGs in MDD and HCs, considering MAGs detected in more than half of the samples of at least one group. As illustrated in Fig. 2C, the node degree was significantly higher in HCs than in the MDD group, while the natural connective was significantly lower in HCs than in the MDD group (Fig. 2D). To assess the resilience of the fragility of the gut microbial co-abundance network, each MAG was removed one by one in order of betweenness rank and degree. The results indicated that the MDD group exhibited the greatest area under the curve, suggesting a more robust co-occurrence network under simulated disruption compared to HCs (Fig. 2E).

To further elucidate the distinct microbial compositions between MDD and HCs, we employed LEfSe analysis to identify 58 MDD-enriched and 46 MDD-reduced

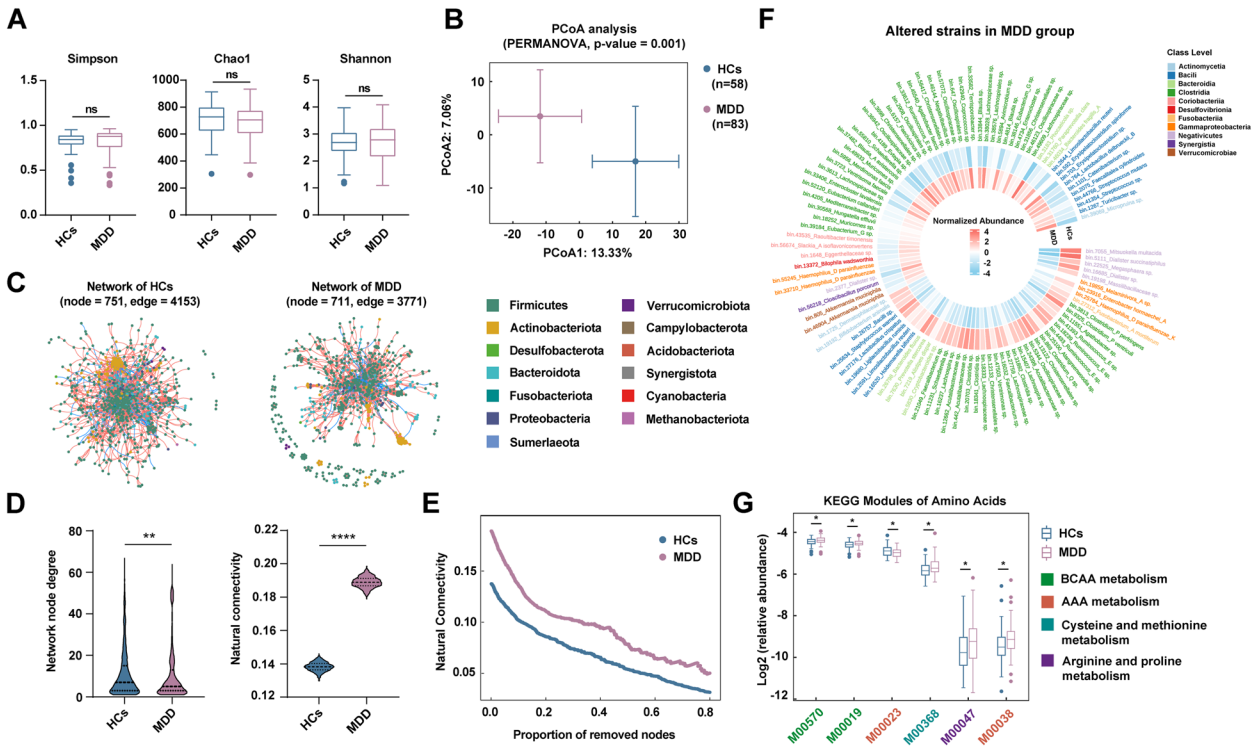

Fig. 2 Specific fecal microbial ecosystem in children and adolescents with MDD. **A** Box and whiskers plots (in the style of Turkey) for the α-diversity analysis of four indices (Simpson, Chao1 and Shannon) at the microbial strain level between MDD patients (n = 83) and HCs (n = 58). **B** Principal component analysis (PCoA) indicates a partial but significant separation between patients with MDD and HCs at microbial strain level. Significance was determined using permutational multivariate analysis of variance (Binomial distance). **C** Visualization of constructed co-occurrence network for the relative abundance of all the 793 metagenome-assembled genomes (MAGs) by using Sparcc in HCs (left) and MDD groups (right). **D** Violin chart demonstrating the connectivity property of the network including network node degree and natural connective (Wilcox test p-value; ** < 0.01, **** < 0.0001). **E** Fragility of the co-occurrence network was measured by the natural connective after removing the nodes. A larger natural connective indicated the corresponding network was more robust/less fragile. **F** The cladogram shows the 104 MAGs were differentially abundant between MDD and HCs by using LEfSe analysis, including 58 up-regulated and 46 down-regulated MAGs in MDD group. **G** Box and whiskers plots (in the style of Turkey) show the 6 MDD-associated microbial Kyoto Encyclopedia of Genes and Genomes (KEGG) modules in amino acids (AAs) pathways between MDD and HCs (Wilcox test p-value; * p-value < 0.05)

strains (p-value < 0.05, LDA > 2; Fig. 2F and TableS12). The majority of the altered MAGs belonged to the class *Clostridia* (Fig. 2F). In accordance with the findings of gut microbiota dysbiosis in adult depression [57], in our adolescent depressed patients we observed the same enrichment of *Eggerthellaceae* bin.1648 that considered to induce inflammation, and reduction of *Faecalibacterium* (bin.16032 and bin.21049) and *Bifidobacterium animalis* (bin.19192), which had been reported to have a function of anti-inflammation and short-chain fatty acid (SCFA) production. Interestingly, *Akkermansia* (bin.805 and bin.46904) exhibited an increase in MDD patients, a phenomenon that has also been observed in individuals with Parkinson's disease [58] and is known to contribute to the production of auto-antigens in patients with IgA nephropathy [59]. A random forest model of the 793 MAGs was applied to measure the importance of microbiota to distinguish MDD and HCs by using mean decrease accuracy (MDA) and mean decrease Gini (MDG) (TableS13). Among the top 30 features based on MDA, 26 of them were overlapped with the significantly different MAGs between MDD and HCs by LEfSe, and all the top 30 features based on MDG also overlapped with the significantly different MAGs between MDD and HCs by LEfSe (the top 30 are shown in Fig.S4). To facilitate the interpretation of MDD-associated microbial functions, of all 474 KEGG modules, 20 were increased, and 20 were decreased in the MDD group (Wilcoxon-Mann–Whitney test, p-value < 0.05; TableS14). Among these modules, we found 8 modules belonged to ATP synthesis that were decreased in the MDD group, and 6 modules in amino acid metabolism were altered in the MDD group, such as aromatic amino acid (AAA) and branched-chain amino acid (BCAA) metabolism (Fig. 2G and TableS14). In summary, these findings demonstrate disturbances in the taxon, co-occurrence networks, and functions of the gut microbiota in children and adolescents with MDD.

Association of gut microbiota and host circulating amino acids in children and adolescents with MDD

Recent literature has reported the involvement of gut bacteria-driven AA or AA derivatives participating in the pathogenesis of depression in adults [12, 13]. To investigate the association between the altered gut microbiome and circulating metabolites in children and adolescents with MDD, we performed Procrustes analysis, which revealed a strong correlation between fecal microbiota and plasma metabolome profiles (p-value = 0.001, M^2 = 0.932; Fig. 3A). Furthermore, the canonical correlation analysis (CCA) identified an association between 66 altered plasma metabolites in amino acid metabolism pathways (TableS15) and 104 altered fecal MAGs (TableS12), indicating that plasma metabolites in amino acid metabolism were clearly separated along the vectors of altered fecal MAGs (Fig. 3B).

Then, a Spearman's correlation analysis was conducted on the MAGs-AAs-symptoms axis in children and adolescents with MDD and HCs. A negative correlation was observed between nine AAs and the total scores of HAMD-24 and HAMA-14, and 72 MAGs demonstrated a significant correlation with at least one AA (Fig. S5). Subsequently, a mediation analysis was conducted to determine the impact of bacterial characteristics on the overall scores of HAMD-24 and HAMA-14, which were influenced by AAs in the metagenome cohort. The inferred causal linkages for the HAMD-24 outcome involved 14 microbial features as initiators and 11 metabolites as mediators (Fig. 3C and TableS16). Similarly, for the HAMA-14 outcome, there were 10 microbial features acting as initiators and 8 metabolites acting as mediators (Fig. 3C and TableS16). For example, the MDD-depleted MAG *Lachnospiraceae* sp. (bin.27759) was identified as an initiator for HAMD-24, with lysine serving as a mediator (Fig. 3D). Besides, the MAGs *Acutalibacteraceae* sp. (bin.442), which was decreased in MDD group, may demonstrate impact on HAMD-24 through plasma methionine (Fig. 3D). Next, we analyzed the gene clusters of AA metabolism in each MAG identified in the mediation analysis. The 15 MAGs identified in the mediation analysis exhibited completed genomes of biosynthesis and degradation modules in amino acid metabolism pathways, including arginine, lysine, tryptophan, phenylalanine, tyrosine, leucine, isoleucine, and methionine (Fig. 3E). Overall, the data suggests a causal inference between alterations in specific gut microbial features, AAs in the host circulation, and the development of depressive or anxious symptoms.

Plasma metabolic alterations associated with prefrontal dysfunction in children and adolescents with MDD

Given the significantly altered plasma metabolic profiles, we next sought to explore whether the plasma metabolic dysregulation is associated with altered brain functional activities in children and adolescents with MDD. First, to characterize the brain functional alterations of children and adolescents with MDD, the whole-brain functional connectivity (FC) of 111 MDD (mean age, 16.3 ± 1.3 years; BMI, 19.8 ± 2.5 kg/m^2; 83 [74.8%] females) was compared with 51 HCs (mean age, 15.4 ± 1.9 years; BMI, 20.1 ± 2.8 kg/m^2; 34 [66.7%] females) (TableS2) using network-based statistics (NBS, MATLAB Toolbox) [60] with adjustment for age, gender, and BMI. The result indicated a single network comprising 29 connections among 27 subregions (FWER corrected p-value = 0.030) significantly differed between MDD and HCs groups (Fig. 4A and Fig. 4B). Specifically, compared with HCs,

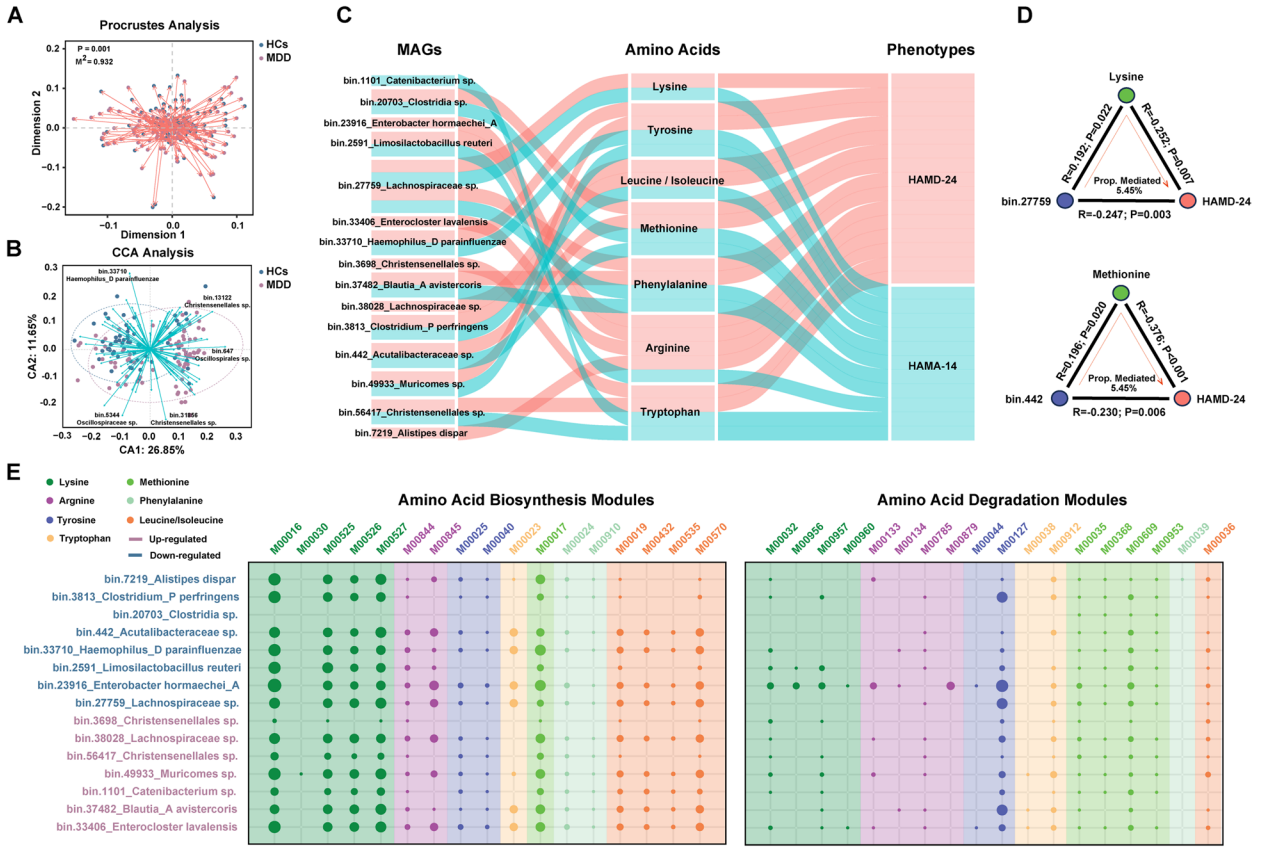

Fig. 3 Interactions of fecal microbial compositions and host circulating amino acids in children and adolescents with MDD. **A** Procrustes analysis of plasma metabolome versus fecal microbiome. Blue and red color of node represent HCs ($n = 58$) and MDD ($n = 83$), respectively. The plasma metabolome and fecal samples from the same individual are connected by red arrows. **B** Canonical correlation analysis (CCA) of the relationships between 66 metabolites related with amino acid metabolism and 104 differentially expressed metagenome-assembled genomes (MAGs). Each MAG is represented with a blue arrow, with the names of the MAGs with the top five distances. Blue and red colors of node represent HCs and MDD, respectively. The sample projections in MAGs and metabolite space are represented by the starting point and the end of the arrow, respectively. **C** Sankey diagram showing the inferred causal relationship network of bacterial features on total scores of 24-item Hamilton Depression Rating Scale (HAMD-24) and the 14-item Hamilton Anxiety Rating Scale (HAMA-14) mediated by amino acids. **D** Examples of inferred causal relationships between microbial features, amino acids and total scores of HAMD-24 and the HAMA-14. **E** Circles represent the presence or absence of amino acid metabolism modules encoded by microbial genomes. The size of each circle indicates the number of genomes within a given bacterial strain encoding enzymes involved in the corresponding metabolic pathway. Colored ranges represent biosynthesis or degradation modules associated with different categories of amino acid pathways

adolescents with MDD manifested significantly reduced functional connectivity of frontal-parietal regions (14/29, 48.3%), particularly involving connections related to the middle frontal gyrus (MFG), superior frontal gyrus (SFG) and superior parietal lobule (SPL). Significant alterations of connections associated with the middle temporal gyrus (MTG) and Hippocampus (Hipp) were also found in adolescents with MDD (TableS17). These results largely align with previous findings [61–63] and further underscore the dysfunctional connectivity implicating prefrontal regions in the neural mechanism of early-onset MDD

Then, by leveraging the connectome-based predictive modeling (CPM) with leave-one-out cross-validation [46], we investigated the linkages between plasma metabolites and brain functional networks. A total of 276 metabolites were found to significantly associate with brain functional networks (p-value < 0.05, r ranged between 0.1551 and 0.4957, NRMSE ranged between 0.0768 and 0.3975), and 72 of which were altered in adolescent depression (Fig. 4C and TableS18), such as lysine, methionine, and cysteine. Notably, AAs accounted for the largest proportion of the FC-related metabolites that were simultaneously implicated in adolescents with MDD (Fig. 4D), suggesting the most regulatory effects of AAs on brain functional activities related to depression.

To map the neural regulatory effects of depression-related AAs, we extracted the FC networks that were

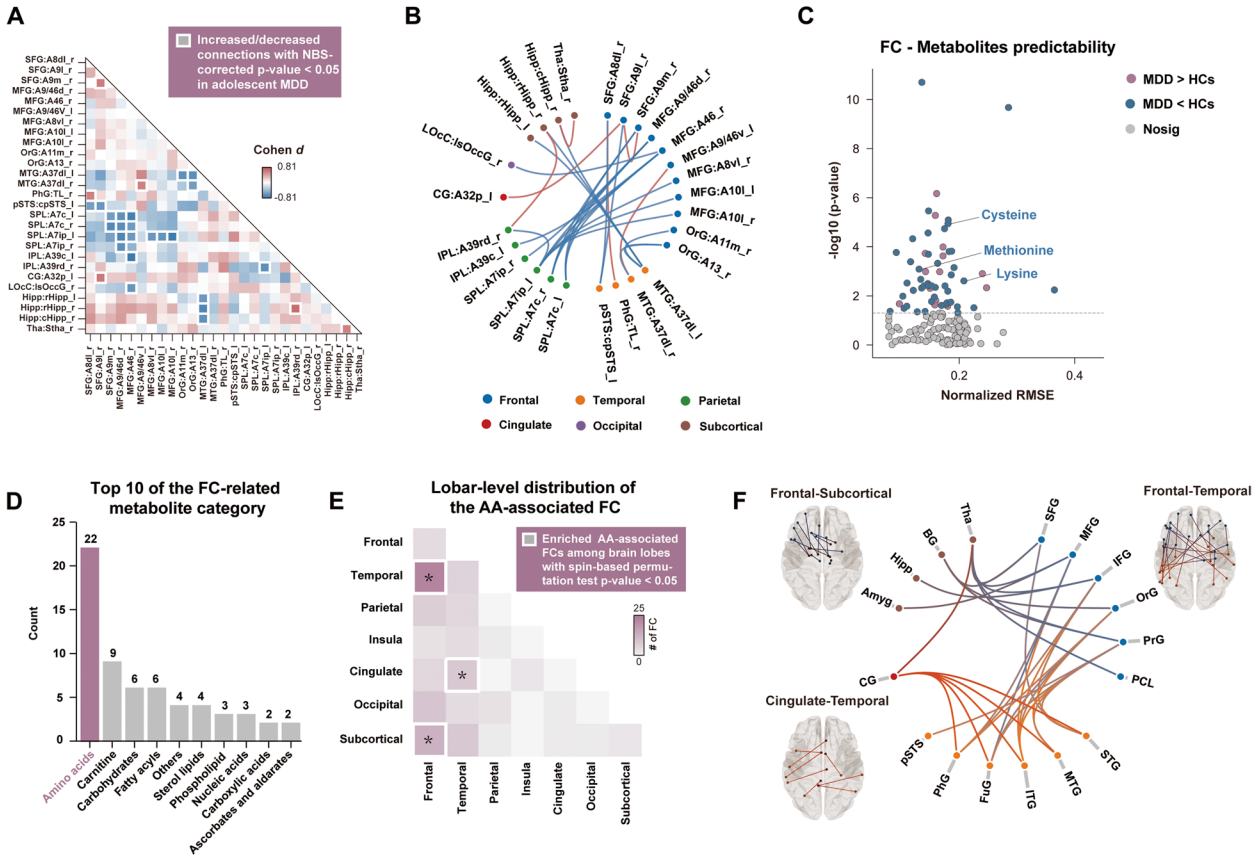

Fig. 4 Depression-related plasma metabolites correlate with brain dysfunction. **A** The group differences of functional connectivity between MDD and HCs in children and adolescents evaluated by network-based statistics (NBS). Grids with white bounding box indicate functional connections that comprise the group-differed network (the family-wise error corrected $p = 0.030$). **B** The group-differed functional connectivity between MDD and HCs in children and adolescents identified via NBS. The linkage between nodes indicates the functional connectivity with significant group differences; the red/blue color of linkage indicates increased (MDD > HC)/decreased (MDD < HC) connections in children and adolescents with MDD; the node color indicates the brain lobe. **C** The predictability of depressive-related metabolites by brain functional connectivity. Significant predictability indicates associations between the metabolites and brain function. The grey dots ($n = 138$) represent metabolites without significant functional connectivity (FC) associations; the red dots ($n = 17$) represent the metabolites with significant FC associations but without group differences between MDD and HCs in children and adolescents. The metabolites that show both significant FC associations and group differences are marked with red (MDD > HCs; $n = 17$)/blue (MDD < HCs; $n = 55$). Only metabolites with positive r are presented (736 out of 1300 metabolites). **D** The count of metabolites belonging to different categories that are both associated with brain function and adolescent depression. Only the top 10 categories are shown. **E** The lobar-level distribution of amino acid (AA)-associated FCs. Grids with white bounding box indicate the lobar-level network enriched with AA-associated FCs identified with spin-based permutation test. *, $p_{spin} < 0.05$. **F** The regional-level distribution of the AA-associated FCs. Only the distributions of the lobar-level networks with significant enrichment of AA-associated FCs are presented. The color linkage in the circle plot and glass brain plot indicates the AA-associated functional connectivity. The node color in the circle plot and glass brain plot indicates the brain lobe. The bar plot around a node indicates the count of AAs with FC associations related to that region. For abbreviations of brain regions, please refer to Table S3, both macro-anatomical and subregional names were presented in the diagram and were separated by a colon

robustly associated with at least one depression-related AAs. At the lobar level (Fig. 4E), we found that the AA-associated FCs were enriched in a frontal–temporal network ($p_{spin} = 0.0358$), frontal-subcortical network ($p_{spin} = 0.0400$), and cingulate-temporal network ($p_{spin} = 0.0100$) via spin-based permutation test. We further illustrated the region-level FC patterns within the three lobar networks enriched for AA-FC linkages (Fig. 4F). Several hub regions that manifested significant dysconnectivity in adolescents with MDD were found to be extensively associated with the depressive-related AAs, particularly including SFG and orbital gyrus in the frontal lobe (Fig. S6). These results highlight the vulnerability of prefrontal functional activity in the face of depression-related AA dysregulation, indicating a potential neural pathway mediating AA dysregulation and MDD in adolescents.

FMT from children and adolescents with MDD induced depressive-like behaviors in adolescent rats accompanied by AAs deficiency in the prefrontal cortex

To further evaluate the potential causal role of the microbiota in AA deficiency and the development of depression in children and adolescents, we transferred microbiota from 19 children and adolescents with MDD or 19 HCs into Abx adolescent rats (Fig. 5A). Following a 7-day adaption period to the housing conditions, all 24 rats aged PND 28 days were administered antibiotic twice daily for 2 weeks. Subsequently, 12 rats in the depression group were colonized with pooled samples of patients with MDD (FMT_MDD), while the remaining rats in the control group were colonized with pooled samples of HCs (FMT_HCs). The bacterial load was similar between FMT_MDD and FMT_HCs groups after FMT (Fig.S7A). After 2 weeks of FMT, the FMT_MDD group exhibited lower body weight (p-value = 0.025, Fig.S7B) and higher depressive-like behaviors, including lower sucrose preference in SPT (p-value = 0.003, Fig. 5B) and higher immobility time in FST (p-value = 0.016, Fig. 5B). No significant differences were observed in the anxiety-like behaviors exhibited by rats in the FMT_HCs and FMT_MDD groups in both EPM (Fig.S7C) and OFT (Fig. S7D).

The scores plot of PCoA of metagenomic sequencing showed a partial but significant global separation between the FMT_HCs and FMT_MDD groups, as well as a closer proximity between donors and recipients within both the MDD and HCs groups at the MAGs level (Fig.S7E). To elucidate MDD-associated microbial functions, 71 out of 273 KEGG modules were linked to MDD, including 42 increased and 29 reduced in FMT_MDD rats (Wilcoxon-Mann–Whitney test, p-value < 0.05; TableS19). Notably, 16 modules related to amino acid metabolism and 15 to energy metabolism showed significant alters in the FMT_MDD group compared to FMT_HCs, mirroring changes observed in the fecal functional modules in MDD patients (Fig.S7F and TableS19). Furthermore, a targeted metabolomic analysis of 20 AAs in the PFC of both FMT_HCs and FMT_MDD groups revealed significant downregulation of 14 AAs in the FMT_MDD group (Fig. 5C and TableS5), with 10 AAs positively correlating with sucrose preference (Fig. 5C). Importantly, most downregulated AAs in the PFC of FMT_MDD rats were also down-regulated in the plasma

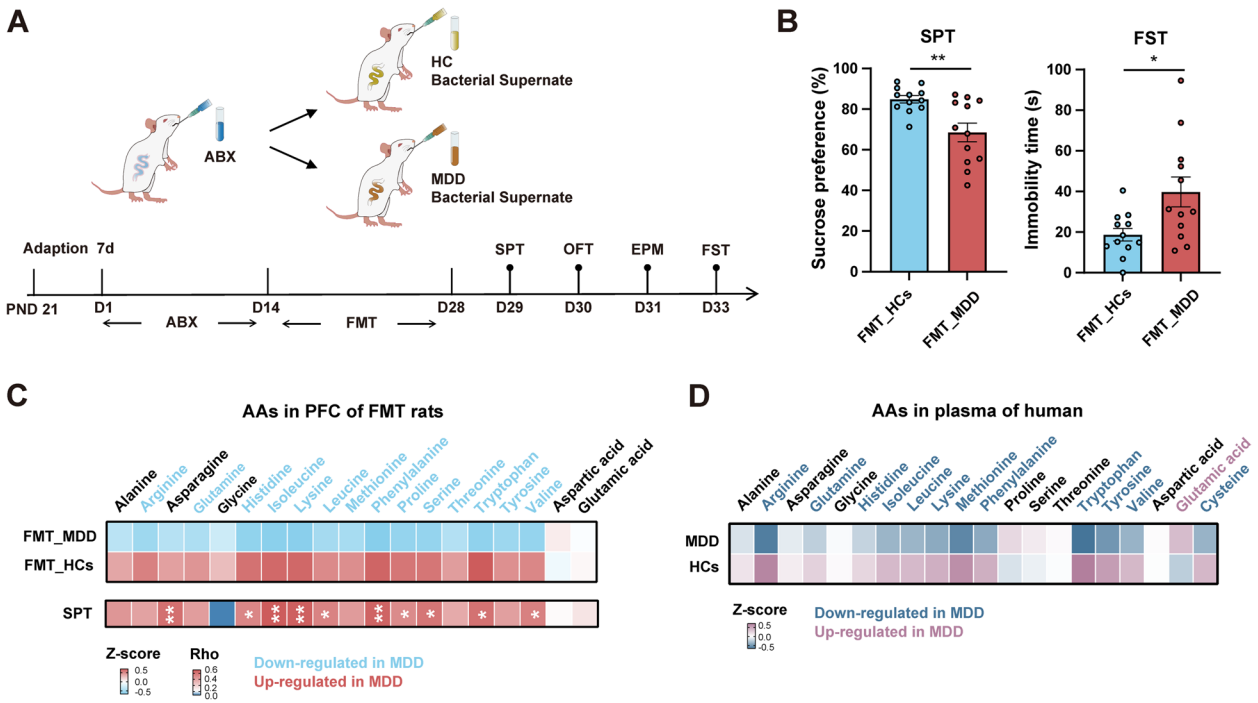

Fig. 5 Fecal microbiota transplantation (FMT) from children and adolescents with MDD-induceddepressive-like behaviors in adolescent rats accompanied by AAs deficiency in the prefrontal cortex (PFC). **A** The experiment schedule of the antibiotic-treated (Abx), FMT and behavioral tests. **B** Lower sucrose preference in sucrose preference test (SPT, left) and higher immobility time in forced swim test (FST, right) was found in FMT_MDD (n = 12) than FMT_HCs (n = 12). Significance was calculated by t-test. **C** The abundances of amino acids in prefrontal cortex of FMT_MDD (n = 8) were significantly lower than FMT_HCs (n = 8), and most of the abundances of amino acids were positively correlated with sucrose preference by Spearman correlation analysis. **D** The down-regulated amino acids (AAs) in plasma of children and adolescents with MDD overlapped with most of the down-regulated AAs in PFC of rats in FMT_MDD group

of children and adolescents with MDD (Fig. 5D and TableS10). In summary, FMT from children and adolescents with MDD induced depressive-like behaviors in adolescent rats, accompanied by deficiencies in AAs in the PFC.

Dietary lysine restriction may increase depression susceptibility in adolescent CUMS rats via modulating EAATs in the PFC

Next, we investigated the specific impact of AA deficiency on the pathogenesis of depression, with particular emphasis on lysine, the most downregulated EAA in the plasma of children and adolescents with MDD (Fig.S8A and TableS10). We employed a CUMS model in adolescent rats subjected to a lysine-restricted diet (containing 70% of the lysine level in the control diet). A total of 34 adolescent rats were randomly assigned to one of four groups: controls with 100% dietary lysine (CON+L100; n=8), controls with 70% dietary lysine (CON+L70; n=8), CUMS with 100% dietary lysine (CUMS+L100; n=9), and CUMS with 70% dietary lysine (CUMS+L70; n=9) (Fig. 6A).

After a 4-week period of stress and dietary lysine restriction, the CUMS+L70 group exhibited lower sucrose preference in the SPT than CUMS+L100 (p-value = 0.026), CON+L70 (p-value < 0.001), and CON+L100 groups (p-value < 0.001) (Fig. 6B). Additionally, the immobility time in FST was significantly increased in the CUMS+L70 group compared to the CUMS+L100 (p-value = 0.041) and CON+L100 groups (p-value < 0.001), whereas no significant difference was observed between CUMS+L70 and CON+L70 groups (p-value = 0.229) (Fig. 6B). All these results suggested that CUMS+L70 group exhibited more pronounced depressive-like behaviors compared to other groups. The body weight of rats in both the CUMS+L100 and CUMS+L70 groups was lower than that of the CON+L100 and CON+L70 groups (all p-value < 0.001). However, there was no significant difference in body weight between the CON+L100 and CON+L70 groups, indicating that dietary lysine restriction did not significantly affect body weight (p-value = 0.997, Fig.S8B). Anxiety-like behaviors, such as time spent in the closed arm of the EPM (Fig.S8C) and total distance and center time in the OFT (Fig.S8D), did not show significant differences among the four groups.

Subsequently, mRNA-seq of the prefrontal cortex (PFC) was conducted across four groups to investigate potential molecular mechanisms. In the comparison of CUMS+L70 vs. CUMS+L100, a total of 1428 differentially expressed genes (DEGs; FDR < 0.05 and FC < 0.67 or > 1.5) were identified, which was significantly higher than the other comparisons: Con+L70 vs. Con+L100 (721 DEGs), CUMS+L100 vs. Con+L100 (63 DEGs), and CUMS+L70 vs. Con+L70 (41 DEGs) (Fig. 6C, TableS20 and Fig.S9). To further elucidate the patterns of DEGs, KEGG enrichment analyses were performed on the PFC for the four comparisons. A total of 77, 73, 34, and 11 KEGG pathways were identified in the comparisons of CUMS+L70 vs. CUMS+L100, Con+L70 vs. Con+L100, CUMS+L100 vs. Con+L100, and CUMS+L70 vs. Con+L70, respectively (p-value < 0.05; TableS21). Among the identified pathways, nine were related to the nervous system (Fig. 6D). Notably, the glutamatergic synapse pathway exhibited significant alterations in the dietary lysine restriction comparisons (CUMS+L70 vs. CUMS+L100 and Con+L70 vs. Con+L100), involving genes encoding glutamate transporters (*slc1a1* and *slc1a2*), also known as excitatory amino acid transporters (EAAT3 and EAAT2, respectively) (TableS21). Recent studies suggest that restoring normal glutamatergic transmission by enhancing glutamate uptake may positively affect depression [64]. Furthermore, downregulated expression of EAAT3 (*slc1a1*) and EAAT2 (*slc1a2*) was observed at both the mRNA (Fig.S10A) and protein levels (Fig. 6E) in the CUMS+L70 group compared to the CUMS+L100 group. Additionally, the expression of EAAT3 (*slc1a1*) and EAAT2 (*slc1a2*) in the PFC was significantly downregulated in the FMT_MDD group, as shown by qRT-PCR (Fig.S10B) and western blot analysis (Fig.S10C). These findings suggested that dietary deficiency of lysine may increase susceptibility to depression in adolescent rats by reducing the expression of EAATs in the PFC.

(See figure on next page.)

Fig. 6 Dietary lysine restriction may increase depression susceptibility in adolescent chronic unpredictable mild stress (CUMS) rats via modulating excitatory amino acid transporters (EAATs) in the prefrontal cortex (PFC). **A** The experiment schedule of the dietary lysine restriction study including four groups: Con+L100 (n = 8), Con+L70 (n = 8), CUMS+L100 (n = 9) and CUMS+L70 (n = 9). PND, postnatal day. SPT, sucrose preference test. OFT, open field test. EPM, elevated plus-maze test. FST, forced swim test. **B** Lower sucrose preference in SPT (left) and higher immobility time in FST (right) was found in CUMS+L70 group than CUMS+L100 and CON+L100 groups. Significance was calculated by Two-way ANOVA. **C** The number of up- and down-regulated differentially expressed genes (DEGs) in four comparisons of CUMS+L70 vs. CUMS+L100, Con+L70 vs. Con+L100, CUMS+L100 vs. Con+L100, and CUMS+L70 vs. Con+L70 (n = 8/group). **D** The DEGs involved Kyoto Encyclopedia of Genes and Genomes (KEGG) pathways in nervous system among four comparisons of CUMS+L70 vs. CUMS+L100, Con+L70 vs. Con+L100, CUMS+L100 vs. Con+L100, and CUMS+L70 vs. Con+L70. **E** Protein expression levels of EAAT2 and EAAT3 in CON+L70, CON+L100, CUMS+L70 and CUMS+L100 (n = 6/group)

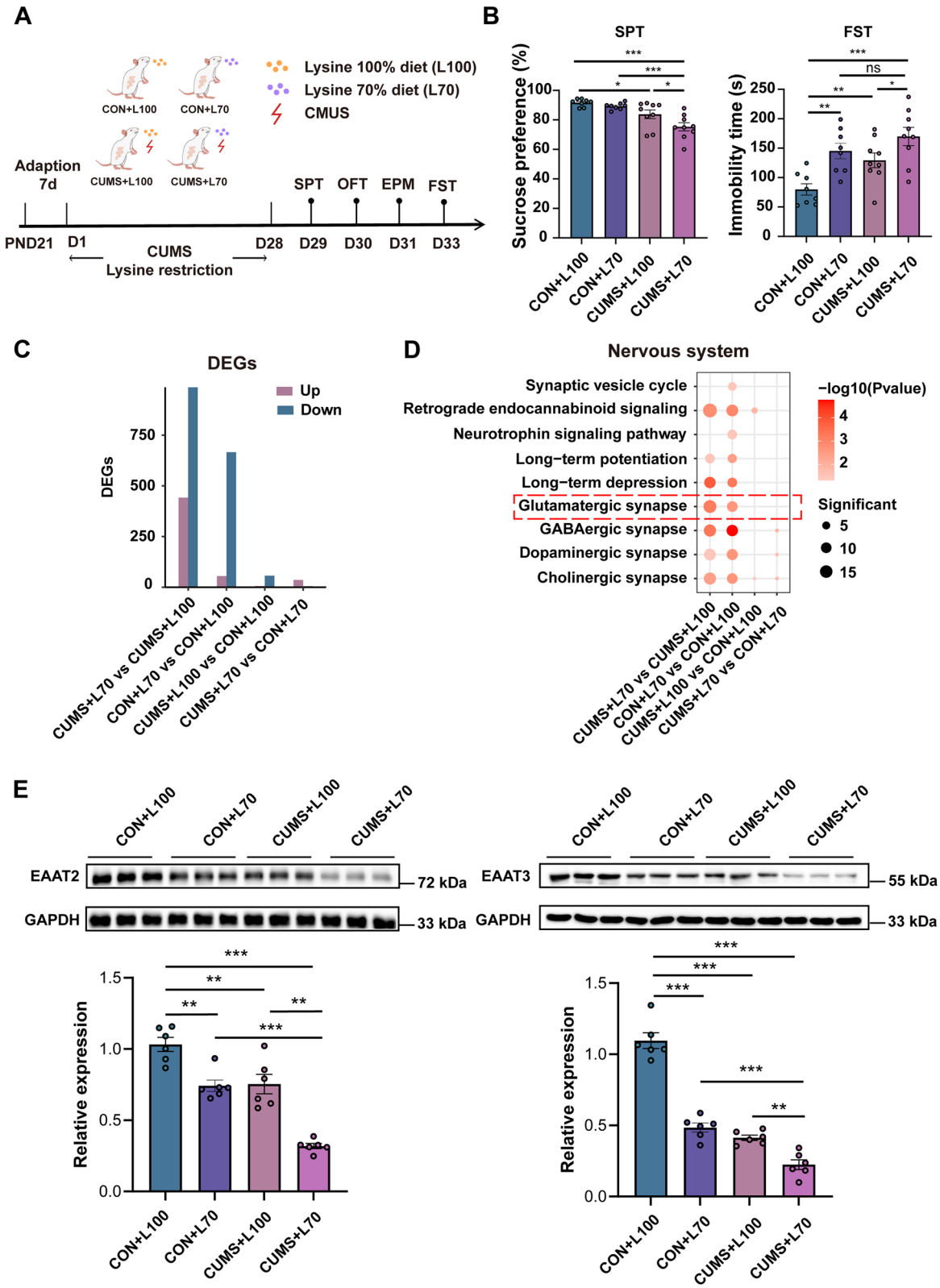

Fig. 6 (See legend on previous page.)

Discussion

Here, we present a comprehensive overview of the MGB axis in children and adolescents with MDD, integrating analysis of the plasma metabolome, gut microbiome, and rs-fMRI. Our findings reveal a significant correlation between the gut microbe-host interactions and the pathogenesis of depression in this demographic, particularly in the context of AA deficiency. Alterations in the gut microbiota associated with depression contribute to AA deficiencies, which in turn disturb the functional connectivity of PFC. Furthermore, FMT from children and adolescents with MDD to adolescent rats also resulted in AA deficiencies in the PFC. Specifically, dietary deficiency of lysine in rats has been shown to reduce the expression of EAAT2 and EAAT3, potentially increasing susceptibility to depression.

The current multi-omics study provided a comprehensive representation of the gut microbiota, plasma metabolome, and resting-state functional connectivity within the MGB axis in the context of depression in children and adolescents. Consistent with previous findings, we observed a depletion of AAs in children and adolescents with MDD [15], suggesting that the high nutritional demands for growth during adolescence may contribute to the pathogenesis of depression. Moreover, adolescence is characterized by substantial hormonal fluctuations, particularly involving the hypothalamic–pituitary–adrenal (HPA) axis and gonadal hormones, which may significantly impact brain connectivity, neurotransmitter synthesis, and gut microbiota composition [65, 66]. While compositional changes in the fecal microbiome have been demonstrated in adult patients with MDD, the gut microbiota of children and adolescents may be more susceptible to environmental factors compared to adults [14]. Two recent studies using 16S rRNA gene sequencing have revealed alterations in the gut microbiota in adolescent depression [67, 68], but this method lacks sufficient taxonomic resolution to report results at the species/strains level and cannot provide direct information on microbial function. In contrast to adult depression, we identified both similar (e.g., *Eggerthella*) and specific (e.g., *Bifidobacterium adolescentis*) altered microbial species in children and adolescents with depression. These altered bacteria, including *Eggerthellaceae*, are considered to induce inflammation, and *Faecalibacterium* has a function of anti-inflammation and butyrate production and has also been widely reported in multiple psychiatric disorders [10]. Notably, we also identified significant disturbances in microbiome functional modules related to amino acid metabolism in this young population with MDD, including AAA metabolism (M00023 and M00038) and arginine and proline metabolism (M00047). These findings align with previous reports indicating their involvement in the pathogenesis of depression [55]. The PFC, a brain region with significantly altered functional connectivity in children and adolescents with MDD, has been identified as impaired in depression [69]. Previous findings suggest that the gut microbiota and metabolites in peripheral blood may influence brain function in patients with depression and bipolar disorders [12, 70]. Altogether, this indicates that the association between gut microbiota and plasma amino acid deficiency may play a role in the pathogenesis of depression in children and adolescents, particularly within the context of the MGB axis.

AAs and AA derivatives (e.g., lysine, kynurenine, and glutamine) have been demonstrated to influence functional connectivity in the PFC in both human and rodent experiments in this study. The tryptophan derivative kynurenine and the neurotransmitter precursor glutamine have also been shown to exhibit decreased levels in multiple psychiatric disorders, including depression [55, 71]. Moreover, kynurenine and glutamine have been extensively documented to play roles in depression via the MGB axis, including in adolescent depression [67, 72]. As early as 2007, a study reported that oral treatment with lysine and arginine reduced anxiety symptoms and basal cortisol levels in a Japanese cohort [73]. The increased nutritional requirements for the rapid growth of the brain during the developmental stages in children and adolescents may result in a lack of AAs [74], which has been associated with adolescents with MDD [75]. Notably, previous studies have reported that *Bifidobacterium animalis*, which was also depleted in adolescents with MDD in our study, can increase fecal lysine levels in individuals with ASD [76]. Recent studies have indicated a potential link between glutaminergic synapse dysfunction and depression, particularly the decreased levels of excitatory amino acid transporters (EAATs), which remove glutamate from the synaptic cleft and transport it into neurons and glia for recycling [77]. Furthermore, human glial-like mesenchymal stem cells, which highly express EAAT, have been demonstrated to improve depressive-like behaviors in a rat model of depression by enhancing glutamate uptake and neurotrophic factor secretion [64]. However, only a few studies have reported the relationship between lysine and the expression of EAATs [78]. Here, our findings suggest that AA alterations, particularly deficiencies in essential amino acids (e.g., lysine), may be involved in glutamatergic synapse dysfunction, which is associated with depression in children and adolescents.

It should be noted that the current study is not without limitations. Firstly, the current study utilized a cross-sectional Chinese cohort of children and adolescents with MDD, which may limit the generalizability of the

findings to longitudinal research or other ethnic groups. Secondly, children and adolescents with MDD in this study were recruited from a specialized clinical center, potentially limiting the representativeness of the sample for the broader population. Our multi-omics findings may also have been influenced by socioeconomic and lifestyle factors, known to significantly impact gut microbiota composition and metabolism. Future studies should incorporate more diverse populations to thoroughly investigate these potential confounding effects. Thirdly, further studies are needed to elucidate the causal relationship between alterations in the specific gut microbiota and amino acid deficiency in the development of depression. Fourthly, despite comprehensive multi-omics analyses, a methodological limitation exists since inference and correlation analyses were conducted on different subsets derived from the initial cohort. This approach could introduce variability and limit the interpretability of direct associations among plasma metabolites, fecal microbiota, and neuroimaging data. Future studies using matched samples across all omics modalities are necessary to strengthen these findings. Fifthly, the behavioral tests employed in our animal models, such as the sucrose preference and forced swim tests, have inherent limitations in their specificity and may not fully capture the complexity of human depressive symptoms. Additionally, the dietary lysine restriction represents a simplified nutritional manipulation; thus, further clinical research involving probiotic supplementation and targeted amino acid interventions in adolescents with depression is needed to enhance translational relevance. Sixthly, although germ-free animals would allow for complete control over baseline microbiota, we opted to use SPF rats to ensure a closer physiological resemblance to conventional hosts, enhancing translational relevance. Lastly, only male rats were included in this study due to known sex differences in gut microbiota, metabolic profiles, and behavioral outcomes, as well as to maintain consistency with prior research that predominantly used male rodents to minimize the confounding effects of hormonal fluctuations. However, future studies should incorporate both male and female models to fully understand sex-specific differences in microbiota-gut-brain interactions and their impact on depression.

In conclusion, our multiple-omics study reveals profound and complex alterations in plasma metabolites, the gut microbiome, and brain functional connectivity in children and adolescents with depression. The gut microbes may act via the MGB axis of amino acid deficiency, affecting depression symptoms in children and adolescents through reduced expression of EAATs in the PFC. Furthermore, our findings indicate that depression susceptibility is heightened in adolescent rats subjected to a lysine deficiency condition, which is also associated with reduced expression of EAATs in the PFC. Our results from multiple-omics analyses of patients and in vivo experiments on rats contribute to our understanding of the causal relationship between the MGB axis and depression in children and adolescents.

Supplementary Information

The online version contains supplementary material available at https://doi.org/10.1186/s40168-025-02122-w.

Supplementary Fig. 1. The overall workflow integrates multiple-omics analyses of patients and in vivo experiments of rats to elucidate the alterations of microbiota-gut-brain (MGB) axis amino acid metabolism in children and adolescents with major depressive disorders (MDD). Related to Fig. 1-6. (A) The plasma samples were collected from a cohort of MDD patients (n=256) and HCs (n=307) in children and adolescents. Fecal samples (subset 1, MDD: n = 83, HCs: n = 58) and rs-fMRI data (subset 2, MDD: n = 111, HCs: n = 51) were obtained from subsets of this cohort. (B) The multi-omics profiles of plasma metabolome, fecal metagenome and brain functional connectivity depicted a landscape MGB axis in children and adolescents with MDD, especially in amino acid metabolism. (C) The integrating multiple-omics was performed to identify the associations between the brain functional connectivity and amino acid metabolism, as well as the causal inference analyses of microbial-amino acids-host links. (D) Experiments on fecal microbiota transplantation (n = 12/group), have shown that we can transfer the microbiota and depressive-like behaviors from humans to adolescent rats, resulting in a similar microbial alterations and depletion of amino acids (AAs) in the prefrontal cortex. (E) Experiments on the dietary lysine restriction (n = 8-9/group), increased the depression susceptibility in adolescent depression model of rats via modulating excitatory amino acid transporters (EAATs) in prefrontal cortex (PFC).

Supplementary Fig. 2. Plasma metabolome analysis in the clinical cohorts. Related to Fig. 1. (A) A clear discrepancy of plasma metabolome between MDD patients (n = 256) and HCs (n = 307), was revealed by Principal Component Analysis (PCA). (B) The receiver operating characteristic (ROC) curve using Components 1, 2, 3 and 4 with 0.998 Area Under the Curve (AUC) to discriminate MDD from HCs in the partial least squares discrimination analysis (PLS-DA) model. (C) Component 4 indicated the lowest classification error rate in the PLS-DA model.

Supplementary Fig. 3. Kyoto Encyclopedia of Genes and Genomes (KEGG) enrichment analysis. Related to Fig. 1, Table S8 and Table S9. (A) KEGG enrichment analysis showing the number of differentially expressed metabolites for KEGG level-2 functional pathways. (B) KEGG enrichment analysis of a total of 360 differentially expressed metabolites for KEGG level-3 functional pathways. The size of the bubble indicates the number of differentially expressed metabolites (DEMs), and the red color indicates the p-value of enrichment analysis. (C) Cross-validation analysis of random forest revealed 8 amino acids (arginine, tryptophan, glutamic acid, methionine, cysteine, tyrosine, lysine and phenylalanine) were combined as panel with the highest accuracy among 13 altered amino acids. (D) The combined panel of 8 amino acids yielded area under the receiver operating characteristic (AUROC) values of 0.978 in the training set.

Supplementary Fig. 4. Random forest model to identify the top 30 importance of metagenome-assembled genomes (MAGs) by using Mean Decrease Accuracy (MDA, left) and Mean Decrease Gini (MDG, right). Related to Fig. 2

Supplementary Fig. 5. Cross-correlation heatmap for the amino acids and clinical information, as well as differentially expressed metagenome-assembled genomes (MAGs) and amino acids. Related to Fig. 3. The red color indicates the positive correlation, and the blue color indicates the negative correlation. * p-value < 0.05, ** p-value < 0.01, *** p-value < 0.001.

Supplementary Fig. 6. The nodal distribution of functional connectivity (FCs) related to amino acids (AAs) implicating in adolescent depression. Related to Fig. 4. The color intensity indicates the count of FCs associated with that macro-scale brain anatomical region, where the within-region count of FCs associated with that macro-scale brain anatomical region, where the within-region associations related to that region. For abbreviations of brain regions, please refer to Table S3

Supplementary Fig. 7. The behavioral tests for fecal microbiota transplantation (FMT) experiments. Related to Fig. 5. (A) The bacterial load was similar between FMT_MDD and FMT_HCs groups after FMT (n = 12/group). (B) Lower body weight was found in FMT_MDD than in FMT_HCs (n = 12/group) at the endpoint (D28). (B) Lower body weight was found in FMT_MDD than in FMT_HCs (n = 12/group) at the endpoint (D28). (D) The center time (left) and the total distance (right) of OFT were not significant between FMT_MDD and FMT_HCs (n = 12/group). (E) Principal component analysis (PCoA) indicates a partial but significant global separation between recipients of MDD patients and HCs, and also reveals a closer distance for donor and recipient in both MDD and HCs groups at MAGs level. Significance was determined using permutational multivariate analysis of variance. (F) Box and whiskers plots (in the style of Turkey) show the 16 MDD-associated microbial Kyoto Encyclopedia of Genes and Genomes (KEGG) modules in AAs pathways between FMT_MDD and FMT_HCs.

Supplementary Fig. 8. The behavioral tests for dietary lysine restriction experiments. Related to Fig. 6. (A) The fold change of essential amino acids (AAs) in the plasma of children and adolescents with MDD. (B) Lower body weight was found in chronic unpredictable mild stress (CUMS) groups (CUMS+L100 and CUMS+L70; n = 9/group) than in control groups (CON+L100 and CON+L70; n = 8/group) at the endpoint (D28). (C) The close-arm time in elevated plus-maze test (EPM) was not significant between four groups. (D) The center time and (left) the total distance (right) in open field test (OFT) was not significant between four groups. Significance was calculated by Two-way ANOVA.

Supplementary Fig. 9. The volcano plot of all the differentially expressed genes (DEGs). Related to Fig. 6. A) DEGs among the comparison of CUMS+L70 vs. CUMS+L100 (n = 5/group). (B) DEGs among the comparison of Con+L70 vs. Con+L100 (n = 5/group). (C) DEGs among the comparison of CUMS+L100 vs. Con+L100 (n = 5/group). (D) DEGs among the comparison of CUMS+L70 vs. Con+L70 (n = 5/group).

Supplementary Fig. 10. The mRNA and protein levels of amino acid transporter 3 (EAAT3, slc1a1) and EAAT2 (slc1a2) in prefrontal cortex (PFC) of rats. Related to Fig. 5 and Fig. 6. (A) The mRNA expression of slc1a1 and slc1a2 in PFC of CON+L70, CON+L100, CUMS+L70 and CUMS+L100 in dietary lysine restriction experiments (n = 6/group). (B) The mRNA expression of slc1a1 and slc1a2 in PFC of FMT_MDD than FMT_HCs (n = 3/group). (C) The protein expression of EAAT2 and EAAT3 in PFC of FMT_MDD than FMT_HCs (n = 10/group).

Supplementary Material 11

Acknowledgements
We thank Dr. Renfu Lai, Rui Zhai and Zhan Chen from Shanghai Adfontes Biotechnology Co., Ltd for their help in analyzing the metabolomics profiling and metagenomic sequencing data.

Authors' contributions
XZ, CZ, and KG designed this study. TT, XL, LGZ, BY, FC, LMZ, and JZ recruited and supervised the participants and performed all clinical procedures. YC and ZJZ performed the preparation, processing, metabolomics profiling of plasma samples. TT and BY performed the preparation, processing, metagenomic sequencing of fecal samples. TT, FH, AG, KG, CZ, and XZ analyzed the metabolomics profiling and metagenomic sequencing data. MX, and JS analyzed the MRI data. TT, BY, LMZ, and JZ performed the experiments of rats. TT, XL, CC, KG, CZ, XY, and XZ prepared the manuscript. All authors approved the manuscript.

Funding
This work was supported by the STI2030-Major Projects (2022ZD0212900), the National Key R&D Program of China (2024YFC2707800), the National Natural Science Foundation of China (82271565, 82301714, 22425404), the China Postdoctoral Science Foundation (2023 TQ0398, GZB20230916, and 2023MD734124), the Natural Science Foundation of Chongqing, China (CSTB2023 NSCQ-BHX0106), the Postdoctoral Innovation Talents Support Program of Chongqing, China (2208013341918508), the Chongqing Medical Young Talent Program (YXQN202499), and the National Key R&D Program of China (2022YFC3400702).

Data availability
The sequence reads of data presented in this manuscript are deposited in the NCBI Short Read Archive (Accession Number: SUB14742785). https://dataview.ncbi.nlm.nih.gov/object/PRJNA1193846?reviewer=5888s0cgq0prhlng843rufamba

Declarations

Ethics approval and consent to participate
This study was approved by the Ethics Committee of the First Affiliated Hospital of Chongqing Medical University. All participants have signed the consent form. All rat experiments were approved by the Institutional Animal Care and Use Committee of Chongqing Medical University.

Consent for publication
Not applicable.

Competing interests
The authors declare no competing interests.

Author details
[1]Department of Psychiatry, Key Laboratory of Major Brain Disease and Aging Research (Ministry of Education), The First Affiliated Hospital of Chongqing Medical University, Chongqing 400014, China. [2]Institute for Brain Science and Disease, Chongqing Medical University, Chongqing 400016, China. [3]State Key Laboratory of Cognitive Neuroscience and Learning, IDG/McGovern Institute for Brain Research, Beijing Normal University, Beijing 100875, China. [4]China Mobile Research Institute, Beijing 100032, China. [5]Interdisciplinary Research Center On Biology and Chemistry, Shanghai Institute of Organic Chemistry, Chinese Academy of Sciences, Shanghai 200032, China. [6]Department of Occupational and Environmental Health, School of Public Health, Chongqing Medical University, Chongqing 400016, China. [7]Research Center for Environment and Human Health, School of Public Health, Chongqing 400016, China. [8]State Key Laboratory of Genetic Engineering, School of Life Sciences, Fudan University, Shanghai 200433, China. [9]Department of Neurology, University of Michigan, Ann Arbor, MI 48109, USA. [10]State Key Laboratory of Microbial Metabolism, School of Life Sciences and Biotechnology, Shanghai Jiao Tong University, Shanghai 200240, China.

Received: 11 November 2024 Accepted: 22 April 2025
Published online: 19 May 2025

References

1. Mokdad AH, Forouzanfar MH, Daoud F, Mokdad AA, El Bcheraoui C, Moradi-Lakeh M, et al. Global burden of diseases, injuries, and risk factors for young people's health during 1990–2013: a systematic analysis for the global burden of disease study 2013. Lancet. 2016;387(10036):2383–401. https://doi.org/10.1016/S0140-6736(16)00648-6.
2. World Health Organization. Depression and other common mental disorders: global health estimates. World Health Organization; 2017. Licence: CC BY-NC-SA 3.0 IGO. https://iris.who.int/bitstream/handle/10665/254610/WHO-MSD-MER-2017.2-eng.pdf?sequence=1.
3. Thapar A, Collishaw S, Pine DS, Thapar AK. Depression in adolescence. Lancet. 2012;379(9820):1056–67. https://doi.org/10.1016/S0140-6736(11)60871-4.
4. World Health Organization. Adolescent and young adult health. 2024. https://www.who.int/newsroom/fact-sheets/detail/adolescents-health-risks-and-solutions.
5. Sarchiapone M, D'Aulerio M, Iosue M. Suicidal ideation, suicide attempts and completed suicide in adolescents: neuro-biological aspects. Biol Aspects Suicidal Behav. 2015;30:11–20.

6. Cipriani A, Zhou X, Del Giovane C, Hetrick SE, Qin B, Whittington C, et al. Comparative efficacy and tolerability of antidepressants for major depressive disorder in children and adolescents: a network meta-analysis. Lancet. 2016;388(10047):881–90. https://doi.org/10.1016/S0140-6736(16)30385-3.
7. Liu S, Gao J, Zhu M, Liu K, Zhang HL. Gut microbiota and dysbiosis in alzheimer's disease: implications for pathogenesis and treatment. Mol Neurobiol. 2020;57(12):5026–43. https://doi.org/10.1007/s12035-020-02073-3.
8. Fan Y, Pedersen O. Gut microbiota in human metabolic health and disease. Nat Rev Microbiol. 2021;19(1):55–71. https://doi.org/10.1038/s41579-020-0433-9.
9. Warner BB. The contribution of the gut microbiome to neurodevelopment and neuropsychiatric disorders. Pediatr Res. 2019;85(2):216–24. https://doi.org/10.1038/s41390-018-0191-9.
10. Nikolova VL, Hall MRB, Hall LJ, Cleare AJ, Stone JM, Young AH. Perturbations in gut microbiota composition in psychiatric disorders: a review and meta-analysis. JAMA Psychiatry. 2021;78(12):1343–54. https://doi.org/10.1001/jamapsychiatry.2021.2573.
11. McGuinness AJ, Davis JA, Dawson SL, Loughman A, Collier F, O'Hely M, et al. A systematic review of gut microbiota composition in observational studies of major depressive disorder, bipolar disorder and schizophrenia. Mol Psychiatry. 2022. https://doi.org/10.1038/s41380-022-01456-3.
12. Zhao M, Ren Z, Zhao A, Tang Y, Kuang J, Li M, et al. Gut bacteria-driven homovanillic acid alleviates depression by modulating synaptic integrity. Cell Metab. 2024;36(5):1000–12 e6. https://doi.org/10.1016/j.cmet.2024.03.010.
13. Mayneris-Perxachs J, Castells-Nobau A, Arnoriaga-Rodríguez M, Martin M, de la Vega-Correa L, Zapata C, et al. Microbiota alterations in proline metabolism impact depression. Cell Metab. 2022;34(5):681–+. https://doi.org/10.1016/j.cmet.2022.04.001.
14. Derrien M, Alvarez AS, de Vos WM. The gut microbiota in the first decade of life. Trends Microbiol. 2019;27(12):997–1010. https://doi.org/10.1016/j.tim.2019.08.001.
15. Zhou X, Liu L, Lan X, Cohen D, Zhang Y, Ravindran AV, et al. Polyunsaturated fatty acids metabolism, purine metabolism and inosine as potential independent diagnostic biomarkers for major depressive disorder in children and adolescents. Mol Psychiatry. 2019;24(10):1478–88. https://doi.org/10.1038/s41380-018-0047-z.
16. Wang H, Jia H, Gao Y, Zhang H, Fan J, Zhang L, et al. Serum metabolic traits reveal therapeutic toxicities and responses of neoadjuvant chemoradiotherapy in patients with rectal cancer. Nat Commun. 2022;13(1):7802. https://doi.org/10.1038/s41467-022-35511-y.
17. Shen X, Wang R, Xiong X, Yin Y, Cai Y, Ma Z, et al. Metabolic reaction network-based recursive metabolite annotation for untargeted metabolomics. Nat Commun. 2019;10(1):1516. https://doi.org/10.1038/s41467-019-09550-x.
18. Zhou Z, Luo M, Zhang H, Yin Y, Cai Y, Zhu ZJ. Metabolite annotation from knowns to unknowns through knowledge-guided multi-layer metabolic networking. Nat Commun. 2022;13(1):6656. https://doi.org/10.1038/s41467-022-34537-6.
19. Chen S, Zhou Y, Chen Y, Gu J. fastp: an ultra-fast all-in-one FASTQ preprocessor. Bioinformatics. 2018;34(17):i884–90. https://doi.org/10.1093/bioinformatics/bty560.
20. Langmead B, Salzberg SL. Fast gapped-read alignment with Bowtie 2. Nat Methods. 2012;9(4):357–9. https://doi.org/10.1038/nmeth.1923.
21. Li D, Liu CM, Luo R, Sadakane K, Lam TW. MEGAHIT: an ultra-fast single-node solution for large and complex metagenomics assembly via succinct de Bruijn graph. Bioinformatics. 2015;31(10):1674–6. https://doi.org/10.1093/bioinformatics/btv033.
22. Hyatt D, Chen GL, Locascio PF, Land ML, Larimer FW, Hauser LJ. Prodigal: prokaryotic gene recognition and translation initiation site identification. BMC Bioinformatics. 2010;11: 119. https://doi.org/10.1186/1471-2105-11-119.
23. Li W, Godzik A. Cd-hit: a fast program for clustering and comparing large sets of protein or nucleotide sequences. Bioinformatics. 2006;22(13):1658–9. https://doi.org/10.1093/bioinformatics/btl158.
24. Li R, Yu C, Li Y, Lam TW, Yiu SM, Kristiansen K, et al. SOAP2: an improved ultrafast tool for short read alignment. Bioinformatics. 2009;25(15):1966–7. https://doi.org/10.1093/bioinformatics/btp336.
25. Buchfink B, Reuter K, Drost HG. Sensitive protein alignments at tree-of-life scale using DIAMOND. Nat Methods. 2021;18(4):366–8. https://doi.org/10.1038/s41592-021-01101-x.
26. Steinegger M, Soding J. MMseqs2 enables sensitive protein sequence searching for the analysis of massive data sets. Nat Biotechnol. 2017;35(11):1026–8. https://doi.org/10.1038/nbt.3988.
27. Kang DD, Li F, Kirton E, Thomas A, Egan R, An H, et al. MetaBAT 2: an adaptive binning algorithm for robust and efficient genome reconstruction from metagenome assemblies. PeerJ. 2019;7: e7359. https://doi.org/10.7717/peerj.7359.
28. Olm MR, Brown CT, Brooks B, Banfield JF. dRep: a tool for fast and accurate genomic comparisons that enables improved genome recovery from metagenomes through de-replication. ISME J. 2017;11(12):2864–8. https://doi.org/10.1038/ismej.2017.126.
29. Parks DH, Imelfort M, Skennerton CT, Hugenholtz P, Tyson GW. CheckM: assessing the quality of microbial genomes recovered from isolates, single cells, and metagenomes. Genome Res. 2015;25(7):1043–55. https://doi.org/10.1101/gr.186072.114.
30. Chaumeil PA, Mussig AJ, Hugenholtz P, Parks DH. GTDB-Tk: a toolkit to classify genomes with the genome taxonomy database. Bioinformatics. 2019;36(6):1925–7. https://doi.org/10.1093/bioinformatics/btz848.
31. Esteban O, Markiewicz CJ, Blair RW, Moodie CA, Isik AI, Erramuzpe A, et al. fMRIPrep: a robust preprocessing pipeline for functional MRI. Nat Methods. 2019;16(1):111–6. https://doi.org/10.1038/s41592-018-0235-4.
32. Gorgolewski K, Burns CD, Madison C, Clark D, Halchenko YO, Waskom ML, et al. Nipype: a flexible, lightweight and extensible neuroimaging data processing framework in python. Front Neuroinform. 2011;5: 13. https://doi.org/10.3389/fninf.2011.00013.
33. Abraham A, Pedregosa F, Eickenberg M, Gervais P, Mueller A, Kossaifi J, et al. Machine learning for neuroimaging with scikit-learn. Front Neuroinform. 2014;8: 14. https://doi.org/10.3389/fninf.2014.00014.
34. Tustison NJ, Avants BB, Cook PA, Zheng Y, Egan A, Yushkevich PA, et al. N4ITK: improved N3 bias correction. IEEE Trans Med Imaging. 2010;29(6):1310–20. https://doi.org/10.1109/TMI.2010.2046908.
35. Zhang Y, Brady M, Smith S. Segmentation of brain MR images through a hidden Markov random field model and the expectation-maximization algorithm. IEEE Trans Med Imaging. 2001;20(1):45–57. https://doi.org/10.1109/42.906424.
36. Fonov VS, Evans AC, McKinstry RC, Almli CR, Collins DL. Unbiased nonlinear average age-appropriate brain templates from birth to adulthood. Neuroimage. 2009;47:S102. https://doi.org/10.1016/S1053-8119(09)70884-5.
37. Avants BB, Epstein CL, Grossman M, Gee JC. Symmetric diffeomorphic image registration with cross-correlation: evaluating automated labeling of elderly and neurodegenerative brain. Med Image Anal. 2008;12(1):26–41. https://doi.org/10.1016/j.media.2007.06.004.
38. Jenkinson M, Bannister P, Brady M, Smith S. Improved optimization for the robust and accurate linear registration and motion correction of brain images. Neuroimage. 2002;17(2):825–41. https://doi.org/10.1016/s1053-8119(02)91132-8.
39. Cox RW, Hyde JS. Software tools for analysis and visualization of fMRI data. NMR Biomed. 1997;10(4–5):171–8. https://doi.org/10.1002/(sici)1099-1492(199706/08)10:4/5%3c171::aid-nbm453%3e3.0.co;2-l.
40. Wang S, Peterson DJ, Gatenby JC, Li W, Grabowski TJ, Madhyastha TM. Evaluation of field map and nonlinear registration methods for correction of susceptibility artifacts in diffusion MRI. Front Neuroinform. 2017;11: 17. https://doi.org/10.3389/fninf.2017.00017.
41. Treiber JM, White NS, Steed TC, Bartsch H, Holland D, Farid N, et al. Characterization and correction of geometric distortions in 814 diffusion weighted images. PLoS One. 2016;11(3): e0152472. https://doi.org/10.1371/journal.pone.0152472.
42. Jenkinson M, Smith S. A global optimisation method for robust affine registration of brain images. Med Image Anal. 2001;5(2):143–56. https://doi.org/10.1016/s1361-8415(01)00036-6.
43. Greve DN, Fischl B. Accurate and robust brain image alignment using boundary-based registration. Neuroimage. 2009;48(1):63–72. https://doi.org/10.1016/j.neuroimage.2009.06.060.
44. Lanczos C. Evaluation of noisy data. J Soc Ind Appl Math Ser B Num Anal. 1964;1:76–85.
45. Power JD, Mitra A, Laumann TO, Snyder AZ, Schlaggar BL, Petersen SE. Methods to detect, characterize, and remove motion artifact in resting

state fMRI. Neuroimage. 2014;84:320–41. https://doi.org/10.1016/j.neuroimage.2013.08.048.
46. Shen X, Finn ES, Scheinost D, Rosenberg MD, Chun MM, Papademetris X, et al. Using connectome-based predictive modeling to predict individual behavior from brain connectivity. Nat Protoc. 2017;12(3):506–18. https://doi.org/10.1038/nprot.2016.178.
47. Xie C, Xiang S, Shen C, Peng X, Kang J, Li Y, et al. A shared neural basis underlying psychiatric comorbidity. Nat Med. 2023;29(5):1232–42. https://doi.org/10.1038/s41591-023-02317-4.
48. Rosenberg MD, Finn ES, Scheinost D, Papademetris X, Shen X, Constable RT, et al. A neuromarker of sustained attention from whole-brain functional connectivity. Nat Neurosci. 2016;19(1):165–71. https://doi.org/10.1038/nn.4179.
49. Vasa F, Seidlitz J, Romero-Garcia R, Whitaker KJ, Rosenthal G, Vertes PE, et al. Adolescent tuning of association cortex in human structural brain networks. Cereb Cortex. 2018;28(1):281–94. https://doi.org/10.1093/cercor/bhx249.
50. Alexander-Bloch AF, Shou H, Liu S, Satterthwaite TD, Glahn DC, Shinohara RT, et al. On testing for spatial correspondence between maps of human brain structure and function. Neuroimage. 2018;178:540–51. https://doi.org/10.1016/j.neuroimage.2018.05.070.
51. Baller EB, Valcarcel AM, Adebimpe A, Alexander-Bloch A, Cui Z, Gur RC, et al. Developmental coupling of cerebral blood flow and fMRI fluctuations in youth. Cell Rep. 2022;38(13): 110576. https://doi.org/10.1016/j.celrep.2022.110576.
52. Li X, Teng T, Yan W, Fan L, Liu X, Clarke G, et al. AKT and MAPK signaling pathways in hippocampus reveals the pathogenesis of depression in four stress-induced models. Transl Psychiatry. 2023;13(1):200. https://doi.org/10.1038/s41398-023-02486-3.
53. Teng T, Clarke G, Maes M, Jiang Y, Wang J, Li X, et al. Biogeography of the large intestinal mucosal and luminal microbiome in cynomolgus macaques with depressive-like behavior. Mol Psychiatry. 2022;27(2):1059–67. https://doi.org/10.1038/s41380-021-01366-w.
54. Gu XY, Ke S, Wang QX, Zhuang TX, Xia CY, Xu Y, et al. Energy metabolism in major depressive disorder: recent advances from omics technologies and imaging. Biomed Pharmacother. 2021;141:ARTN 111869. https://doi.org/10.1016/j.biopha.2021.111869.
55. Pu JC, Liu YY, Zhang HP, Tian L, Gui SW, Yu Y, et al. An integrated meta-analysis of peripheral blood metabolites and biological functions in major depressive disorder. Mol Psychiatry. 2021;26(8):4265–76. https://doi.org/10.1038/s41380-020-0645-4.
56. Dalangin R, Kim A, Campbell RE. The role of amino acids in neurotransmission and fluorescent tools for their detection. Int J Mol Sci. 2020;21(17):ARTN 6197. https://doi.org/10.3390/ijms21176197.
57. Liu LX, Wang HY, Zhang HP, Chen XY, Zhang YD, Wu J, et al. Toward a deeper understanding of gut microbiome in depression: the promise of clinical applicability. Adv Sci. 2022;9(35). https://doi.org/10.1002/advs.202203707.
58. Nishiwaki H, Ito M, Ishida T, Hamaguchi T, Maeda T, Kashihara K, et al. Meta-analysis of gut dysbiosis in Parkinson's disease. Mov Disord. 2020;35(9):1626–35. https://doi.org/10.1002/mds.28119.
59. Gleeson PJ, Benech N, Chemouny J, Metallinou E, Berthelot L, da Silva J, et al. The gut microbiota posttranslationally modifies IgA1 in autoimmune glomerulonephritis. Sci Transl Med. 2024;16(740):eadl6149. https://doi.org/10.1126/scitranslmed.adl6149.
60. Zalesky A, Fornito A, Bullmore ET. Network-based statistic: identifying differences in brain networks. Neuroimage. 2010;53(4):1197–207. https://doi.org/10.1016/j.neuroimage.2010.06.041.
61. Kaiser RH, Andrews-Hanna JR, Wager TD, Pizzagalli DA. Large-scale network dysfunction in major depressive disorder: a meta-analysis of resting-state functional connectivity. JAMA Psychiatry. 2015;72(6):603–11. https://doi.org/10.1001/jamapsychiatry.2015.0071.
62. Ho TC, Connolly CG, Henje Blom E, LeWinn KZ, Strigo IA, Paulus MP, et al. Emotion-dependent functional connectivity of the default mode network in adolescent depression. Biol Psychiatry. 2015;78(9):635–46. https://doi.org/10.1016/j.biopsych.2014.09.002.
63. Zheng R, Chen Y, Jiang Y, Zhou B, Han S, Wei Y, et al. Abnormal voxel-wise whole-brain functional connectivity in first-episode, drug-naive adolescents with major depression disorder. Eur Child Adolesc Psychiatry. 2023;32(7):1317–27. https://doi.org/10.1007/s00787-022-01959-y.
64. Shwartz A, Betzer O, Kronfeld N, Kazimirsky G, Cazacu S, Finniss S, et al. Therapeutic effect of astroglia-like mesenchymal stem cells expressing glutamate transporter in a genetic rat model of depression. Theranostics. 2017;7(10):2690–703. https://doi.org/10.7150/thno.18914.
65. Vigil P, Del Rio JP, Carrera B, ArAnguiz FC, Rioseco H, Cortes ME. Influence of sex steroid hormones on the adolescent brain and behavior: an update. Linacre Q. 2016;83(3):308–29. https://doi.org/10.1080/00243639.2016.1211863.
66. Flannery J, Callaghan B, Sharpton T, Fisher P, Pfeifer J. Is adolescence the missing developmental link in microbiome-gut-brain axis communication? Dev Psychobiol. 2019;61(5):783–95. https://doi.org/10.1002/dev.21821.
67. Zhou M, Fan Y, Xu L, Yu Z, Wang S, Xu H, et al. Microbiome and tryptophan metabolomics analysis in adolescent depression: roles of the gut microbiota in the regulation of tryptophan-derived neurotransmitters and behaviors in human and mice. Microbiome. 2023;11(1):145. https://doi.org/10.1186/s40168-023-01589-9.
68. Thapa S, Sheu JC, Venkatachalam A, Runge JK, Luna RA, Calarge CA. Gut microbiome in adolescent depression. J Affect Disord. 2021;292:500–7. https://doi.org/10.1016/j.jad.2021.05.107.
69. Pizzagalli DA, Roberts AC. Prefrontal cortex and depression. Neuropsychopharmacology. 2022;47(1):225–46. https://doi.org/10.1038/s41386-021-01101-7.
70. Li Z, Lai J, Zhang P, Ding J, Jiang J, Liu C, et al. Multi-omics analyses of serum metabolome, gut microbiome and brain function reveal dysregulated microbiota-gut-brain axis in bipolar depression. Mol Psychiatry. 2022;27(10):4123–35. https://doi.org/10.1038/s41380-022-01569-9.
71. Fernandes B, Marx W, McGuinness A, Diaz AP, Soares J. The kynurenine pathway in major depressive disorder, bipolar disorder, and schizophrenia: a meta-analysis of 101 studies. Neuropsychopharmacology. 2020;45(Suppl 1):101–2.
72. Onaolapo AY, Onaolapo OJ. Glutamate and depression: reflecting a deepening knowledge of the gut and brain effects of a ubiquitous molecule. World J Psychiatr. 2021;11(7):297–315. https://doi.org/10.5498/wjp.v11.i7.297.
73. Smriga M, Ando T, Akutsu M, Furukawa Y, Miwa K, Morinaga Y. Oral treatment with L-lysine and L-arginine reduces anxiety and basal cortisol levels in healthy humans. Biomed Res. 2007;28(2):85–90. https://doi.org/10.2220/biomedres.28.85.
74. Chopra C, Mandalika S, Kinger N. Does diet play a role in the prevention and management of depression among adolescents? A narrative review. Nutr Health. 2021;27(2):243–63. https://doi.org/10.1177/0260106020980532.
75. Wang L, Yang P, Yang C, Yang D, Wu X, Cao T, et al. Disturbance of neurotransmitter metabolism in drug-naive, first-episode major depressive disorder: a comparative study on adult and adolescent cohorts. Eur Arch Psychiatry Clin Neurosci. 2022;272(7):1283–96. https://doi.org/10.1007/s00406-022-01406-8.
76. Li Y, Hu W, Lin B, Ma T, Zhang Z, Hu W, et al. Omic characterizing and targeting gut dysbiosis in children with autism spectrum disorder: symptom alleviation through combined probiotic and medium-carbohydrate diet intervention - a pilot study. Gut Microbes. 2024;16(1): 2434675. https://doi.org/10.1080/19490976.2024.2434675.
77. Veeraiah P, Noronha JM, Maitra S, Bagga P, Khandelwal N, Chakravarty S, et al. Dysfunctional glutamatergic and gamma-aminobutyric acidergic activities in prefrontal cortex of mice in social defeat model of depression. Biol Psychiatry. 2014;76(3):231–8. https://doi.org/10.1016/j.biopsych.2013.09.024.
78. Liu L, Zhang S, Bao J, He X, Tong D, Chen C, et al. Melatonin improves laying performance by enhancing intestinal amino acids transport in hens. Front Endocrinol (Lausanne). 2018;9: 426. https://doi.org/10.3389/fendo.2018.00426.

Publisher's Note